arXiv:1911.04632v2 [physics.ins-det] 3 Apr 2020

EUROPEAN ORGANISATION FOR NUCLEAR RESEARCH (CERN)

JINST 15 (2020) P04003
DOI: 10.1088/1748-0221/15/04/P04003

CERN-EP-2019-207
1st February 2022

ATLAS data quality operations and performance for 2015–2018 data-taking

The ATLAS Collaboration

The ATLAS detector at the Large Hadron Collider reads out particle collision data from over 100 million electronic channels at a rate of approximately 100 kHz, with a recording rate for physics events of approximately 1 kHz. Before being certified for physics analysis at computer centres worldwide, the data must be scrutinised to ensure they are clean from any hardware or software related issues that may compromise their integrity. Prompt identification of these issues permits fast action to investigate, correct and potentially prevent future such problems that could render the data unusable. This is achieved through the monitoring of detector-level quantities and reconstructed collision event characteristics at key stages of the data processing chain. This paper presents the monitoring and assessment procedures in place at ATLAS during 2015–2018 data-taking. Through the continuous improvement of operational procedures, ATLAS achieved a high data quality efficiency, with 95.6% of the recorded proton-proton collision data collected at $\sqrt{s}$ = 13 TeV certified for physics analysis.

© 2022 CERN for the benefit of the ATLAS Collaboration.
Reproduction of this article or parts of it is allowed as specified in the CC-BY-4.0 license.

Contents

1 Introduction **2**

2 ATLAS detector **3**

3 Data quality infrastructure and operations **4**

4 Data quality monitoring and assessment **9**
4.1 Data quality defects 9
4.2 Online data quality monitoring 10
4.3 Data quality assessment 11

5 Data quality performance **16**

6 Summary **23**

1 Introduction

The ATLAS detector [1] at the CERN Large Hadron Collider (LHC) [2] is a multipurpose particle detector, optimised to exploit the full physics potential of high-energy proton–proton (pp) and heavy-ion collisions. This includes the study of the Higgs boson, precise measurements of Standard Model processes, searches for rare and new phenomena, as well as the study of the properties and states of matter at high temperatures. ATLAS has over 100 million electronic channels, which provide read-out for multiple, distinct detector subsystems, each featuring dedicated technologies to serve a specific purpose. During data-taking it is important that data are available from all detector subsystems, and that they are free from integrity issues. It is possible that data from one or more individual detector components may occasionally be compromised. This could happen, for example, as a result of a surge in noise from detector electronics or from a high-voltage trip in a detector module. In order to ensure that data provided for physics analysis are of sufficient quality, any such issues must be identified, with data collected during the affected time period being marked appropriately. Thus, data collected during these periods of transient detector issues can be excluded from analyses. To achieve this, the data collected by each detector subsystem are constantly monitored and their conditions recorded, with automated procedures in place where appropriate. Communication with detector operation, software, and hardware experts is important to provide a constant feedback loop, so that the capacity for effectively identifying, preventing or treating data quality (DQ) issues is continuously improved. The final decision on whether or not data are usable is based on scrutiny of the relevant issues by a team of experts.

ATLAS began collecting pp collision data at $\sqrt{s} = 13$ TeV in mid-2015, marking the start of the LHC Run 2 data-taking campaign. During the following four-year experimental programme that ran until the end of 2018, the DQ monitoring procedures, built on the tools and experience developed during Run 1, were constantly revised and improved. This, combined with advances in detector operational procedures, resulted in the DQ efficiency increasing year by year. This paper presents the DQ assessment procedures in place at ATLAS during Run 2, and the DQ performance achieved as a result. The paper is organised as follows. The ATLAS detector is described in Section 2, and an overview of DQ operations and infrastructure is given in Section 3, where DQ-related tools and applications are introduced. Following this, the usage of

these tools in the context of DQ monitoring and assessment is given in Section 4. Here the DQ workflow, as performed during Run 2 data-taking, is described. The performance of these practices and resulting DQ efficiencies are presented and discussed in Section 5, with a closing summary provided in Section 6.

2 ATLAS detector

The ATLAS detector at the LHC covers nearly the entire solid angle around the collision point.[1] It consists of an inner tracking detector surrounded by a thin superconducting solenoid, electromagnetic and hadronic calorimeters, and a muon spectrometer incorporating three large superconducting toroidal magnets.

The inner detector (ID) system is immersed in a 2 T axial magnetic field and provides charged-particle tracking in the range $|\eta| < 2.5$. The high-granularity silicon pixel detector covers the vertex region and typically provides four measurements per track, the first hit being normally in the insertable B-layer (IBL), installed before Run 2 [3, 4]. It is followed by the semiconductor tracking detector (SCT), which is based on silicon microstrips and usually provides eight measurements per track. These subsystems are crucial for the reconstruction of charged-particle tracks, the accuracy of which is limited by the finite resolution of the detector elements and incomplete knowledge of their positions. The silicon detectors are complemented by the transition radiation tracker (TRT), which enables radially extended track reconstruction up to $|\eta| = 2.0$. The TRT also provides electron identification information based on the number of hits (typically 30 in total) above an energy-deposit threshold corresponding to transition radiation. The ID system provides essential information for the reconstruction of *physics objects* such as electrons [5], muons [6], τ-leptons [7], photons [5] and jets [8], as well as for identification of jets containing b-hadrons [9], and for event-level quantities that use charged-particle tracks as input.

The calorimeter system covers the pseudorapidity range $|\eta| < 4.9$. Within the region $|\eta| < 3.2$, electromagnetic calorimetry is provided by barrel and endcap high-granularity lead/liquid-argon (LAr) calorimeters, with an additional thin LAr presampler covering $|\eta| < 1.8$, to correct for energy loss in material upstream of the calorimeters. Hadronic calorimetry is provided by the steel/scintillator-tile calorimeter, segmented into three barrel structures within $|\eta| < 1.7$, and two copper/LAr hadronic endcap calorimeters. The solid angle coverage is completed with forward copper/LAr and tungsten/LAr calorimeter modules optimised for electromagnetic and hadronic measurements, respectively. The calorimeters play an important role in the reconstruction of physics objects such as photons, electrons, τ-leptons and jets, as well as event-level quantities such as missing transverse momentum [10].

The muon spectrometer (MS) comprises separate trigger and high-precision tracking chambers measuring the deflection of muons in a magnetic field generated by superconducting air-core toroids. The field integral of the toroids ranges between 2.0 and 6.0 T m across most of the detector. A set of precision chambers covers the region $|\eta| < 2.7$ with three layers of monitored drift tubes (MDTs), complemented by cathode strip chambers (CSCs) in the forward region, where the background is highest. The muon trigger system covers the range $|\eta| < 2.4$ with resistive-plate chambers (RPCs) in the barrel, and thin-gap chambers (TGCs) in the endcap regions.

[1] ATLAS uses a right-handed coordinate system with its origin at the nominal interaction point (IP) in the centre of the detector and the z-axis along the beam pipe. The x-axis points from the IP to the centre of the LHC ring, and the y-axis points upwards. Cylindrical coordinates (r, ϕ) are used in the transverse plane, ϕ being the azimuthal angle around the z-axis. The pseudorapidity is defined in terms of the polar angle θ as $\eta = -\ln\tan(\theta/2)$.

Interesting events are selected to be recorded by the first-level (L1) trigger system implemented in custom hardware, followed by selections made by algorithms implemented in software in the high-level trigger (HLT) [11]. The L1 trigger makes decisions at the 40 MHz bunch crossing rate and accepts events at a rate below 100 kHz, which the HLT further reduces in order to record complete physics events to disk at about 1 kHz. The trigger system makes use of physics object- or event-level selections using information from the detector subsystems; hence issues affecting detector components can impact the trigger performance downstream. Comprehensive monitoring of trigger rates, detector status and physics object quality is therefore imperative to enable the identification of operational issues in real time.

The reconstruction of physics objects requires input from a combination of detector subsystems. To monitor physics object quality, expertise is required in both the combination of detector information used in reconstruction, and the algorithms that facilitate this. *Combined performance* experts work in collaboration with dedicated subsystem and trigger experts to ensure scrutiny at every level.

3 Data quality infrastructure and operations

The ATLAS experiment began taking 13 TeV pp collision data with a nominal bunch-spacing of 50 ns in July 2015, before the LHC progressed to the design 25 ns bunch-spacing one month later. The latter is the main data-taking mode during Run 2, referred to hereafter as the "standard" Run 2 configuration (in which the "standard" Run 2 dataset was collected). In addition to this, the four years were interspersed with special data-taking periods, with the LHC providing collision data in different machine configurations. Such periods include, for example, instances where the LHC collides heavy ions, periods in which the proton centre-of-mass energy is lower than the nominal 13 TeV, or periods during which the mean number of interactions per bunch crossing,[2] μ, is lowered to $\mu = 2$. The luminosity-weighted μ distribution for the full Run 2 pp collision $\sqrt{s} = 13$ TeV dataset is shown in Figure 1, where the $\mu = 2$ periods can be seen at the left end of the figure. A summary of the main data-taking campaigns for 2015–2018 considered in this paper is presented in Table 1. Other special data-taking periods and configurations that are not discussed herein include machine commissioning periods, detector calibration or van der Meer (vdM) beam separation scans for luminosity calibration [12], very-low-μ data-taking for forward physics programmes, and data-taking with high β^* [13]. During 2018, short vdM-like scans (called *emittance scans*) were performed during standard physics data-taking at ATLAS in addition to dedicated vdM scans. Since emittance scans take place during standard pp data-taking, they are included as a part of the standard Run 2 dataset in this paper, although data collected during an emittance scan are not used for typical physics analyses (as discussed further in Section 5). The uncertainty in the integrated luminosity of the standard Run 2 dataset is 1.7% [12], obtained using the LUCID-2 detector [14] for the primary luminosity measurements.

A single uninterrupted period with beams circulating in the LHC machine is called a *fill*. Typically ATLAS records data continuously during a single LHC fill. Data-taking for physics begins as soon as possible after the LHC declares "stable beams",[3] a condition indicating that stable particle collisions have been achieved. At this point there is high-voltage (HV) ramp up in the Pixel, SCT, and muon system. Once

[2] The mean number of interactions per crossing corresponds to the mean of the Poisson distribution of the number of interactions per crossing calculated for each proton bunch. It is calculated from the instantaneous luminosity per bunch as $\mu = L_{\text{bunch}} \times \sigma_{\text{inel}} / f_{\text{r}}$, where L_{bunch} is the per bunch instantaneous luminosity, σ_{inel} is the inelastic cross section (which is taken to be 80 mb for 13 TeV collisions), and $f_{\text{r}} = 11245.5$ Hz is the LHC revolution frequency.

[3] The timestamp that marks the start of "stable beams" is determined from the LHC General Machine Timing hardware signal.

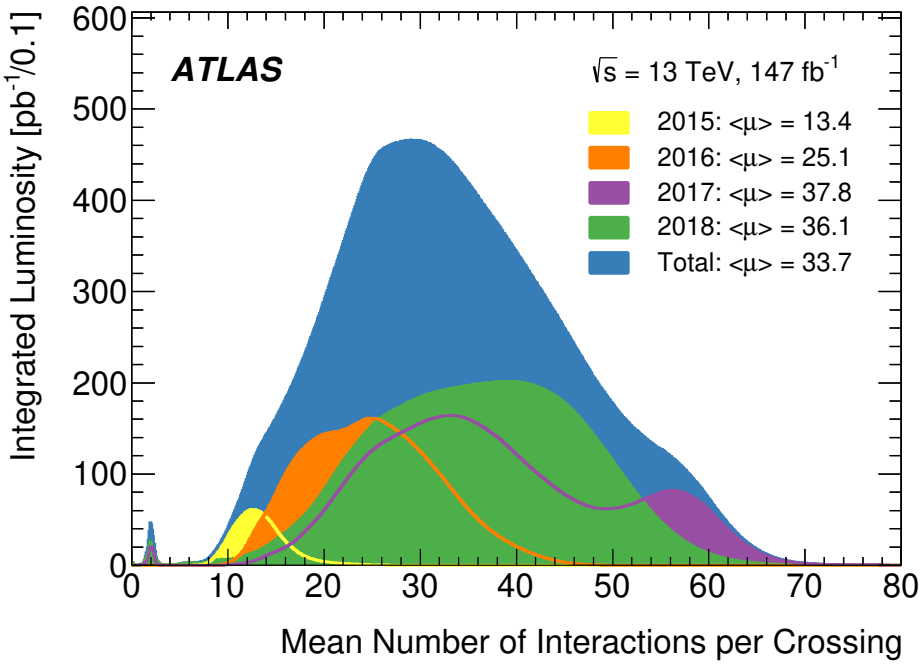


Figure 1: Luminosity-weighted distribution of the mean number of interactions per bunch crossing, μ, for the full Run 2 pp collision dataset at $\sqrt{s}$ = 13 TeV. The μ corresponds to the mean of the Poisson distribution of the number of interactions per crossing calculated for each proton bunch. It is calculated from the instantaneous per bunch luminosity. All data recorded by ATLAS during stable beams are shown, including machine commissioning periods, special runs for detector calibration, LHC fills with a low number of circulating bunches or bunch spacing greater than 25 ns. The integrated luminosity and the mean μ value for each year are given also.

the preamplifiers of the pixel system are turned on, ATLAS is declared "ready for physics". Each of the datasets taken while ATLAS is continuously recording is referred to as an ATLAS *run*, with each individual run being assigned a unique six-digit run number. Each run is further divided into *luminosity blocks* (LBs). An LB is a period of time during which instantaneous luminosity, detector and trigger configuration and data quality conditions are considered constant. In general one LB corresponds to a time period of 60 s, although LB duration is flexible and actions that might alter the run configuration or detector conditions trigger the start of a new LB before 60 s have elapsed. LB start and end timestamps are assigned in real time during data-taking by the ATLAS Central Trigger Processor [15]. The LB serves as a standard unit of granularity for data quality book-keeping. Despite this, rejection of inferior-quality data is possible at a much finer granularity (either event-by-event or within O(ms) "time windows") provided that the grounds and associated parameters are identified in time to be taken into account during the data reconstruction, as described further in Section 4.

Detector and trigger status, configuration, and other time-dependent information such as calibration constants, called detector *conditions* [16], are stored in the ATLAS conditions database [17]. This is an Oracle database hosting a COOL technology schema [18], which allows the storing of conditions data according to an *interval of validity* (IOV). The IOV has a start and end timestamp (in ns), or run and luminosity block identifier, between which the stored conditions are valid and applicable to the data. Given that LB length is not fixed, the timestamps that mark the start and end of each LB are also stored in the

Table 1: Summary of the main data-taking campaigns of each year during Run 2, along with the corresponding delivered and recorded integrated luminosities. The integrated luminosity of the data delivered to ATLAS by the LHC between the time at which the LHC has declared "stable beams" and the point when sensitive subsystems are switched off to allow a beam dump or beam studies is typically defined as the "delivered" luminosity. The subset of these data that is recorded by ATLAS is defined as the "recorded" luminosity. The corresponding centre-of-mass energy is also given alongside each dataset, where $\sqrt{s_{NN}}$ is the centre-of-mass energy per nucleon pair in the case of heavy-ion data-taking periods.

Year	Dataset	Integrated Luminosity	
		Delivered	Recorded
2015	pp @ $\sqrt{s}$ = 13 TeV (50 ns)	102.2 pb^{-1}	94.5 pb^{-1}
	pp @ $\sqrt{s}$ = 13 TeV (25 ns)	3.88 fb^{-1}	3.63 fb^{-1}
	pp @ $\sqrt{s}$ = 5.02 TeV	26.1 pb^{-1}	25.6 pb^{-1}
	Pb-Pb @ $\sqrt{s_{NN}}$ = 5.02 TeV	0.51 nb^{-1}	0.50 nb^{-1}
2016	pp @ $\sqrt{s}$ = 13 TeV	38.0 fb^{-1}	35.5 fb^{-1}
	p-Pb @ $\sqrt{s_{NN}}$ = 8.16 TeV	170 nb^{-1}	167 nb^{-1}
	p-Pb @ $\sqrt{s_{NN}}$ = 5.02 TeV	0.44 nb^{-1}	0.43 nb^{-1}
2017	pp @ $\sqrt{s}$ = 13 TeV	49.0 fb^{-1}	46.4 fb^{-1}
	Xe-Xe @ $\sqrt{s_{NN}}$ = 5.44 TeV	1.97 nb^{-1}	1.96 nb^{-1}
	pp @ $\sqrt{s}$ = 5.02 TeV (μ = 2)	273 pb^{-1}	270 pb^{-1}
	pp @ $\sqrt{s}$ = 13 TeV (μ = 2)	150 pb^{-1}	148 pb^{-1}
2018	pp @ $\sqrt{s}$ = 13 TeV	62.1 fb^{-1}	60.0 fb^{-1}
	pp @ $\sqrt{s}$ = 13 TeV (μ = 2)	213 pb^{-1}	208 pb^{-1}
	Pb-Pb @ $\sqrt{s_{NN}}$ = 5.02 TeV	1.78 nb^{-1}	1.74 nb^{-1}

conditions database.

A number of online applications are responsible for recording the status of conditions in the conditions database. Here "online" refers to services that run during real-time data-taking at ATLAS, while "offline" applications are run during data reconstruction at Tier 0.[4] The operational status of detector hardware components is controlled and monitored by the Detector Control System (DCS) [20], providing information that includes component temperatures, high-voltage values and operational capacity. Further monitoring of low-level detector information is provided by GNAM [21, 22], a lightweight tool that monitors detector status at various stages of the data-flow [23], creating monitoring histograms. During data-taking the trigger system also constantly monitors the data passed by the L1 trigger, including data that are not subsequently recorded to disk. This ensures that interesting events are not unintentionally discarded, and that the HLT algorithms are operating as expected. In addition, the HLT system generates a set of histograms that monitor aspects of its operation. For monitoring of higher-level information, including the quality of reconstructed physics objects, full event reconstruction is run on a small subset of trigger-accepted events and histograms are produced with code similar to that used for monitoring during the offline processing. Automated checks are carried out on the produced histograms using the Data Quality Monitoring Framework (DQMF) [24]. These checks are described in detail in Section 4.2. The algorithms that run in the DQMF must be lightweight such that they comply with data-processing time restrictions and must be written and tested offline, independently of online data-taking. This means that the DQMF is compatible with the online

[4] ATLAS uses the Worldwide LHC Computing Grid (WLCG) [19] to store and reconstruct data. The WLCG defines a hierarchical "Tier" structure for computing infrastructure: ATLAS uses the Tier 0 farm at CERN for initial (prompt) reconstruction of the recorded data; later data reprocessing proceeds primarily on the eleven Tier 1 sites.

and offline environments, and its use in the two environments differs only in the methods used to deliver histograms to the framework and publish the results.

The Information Service (IS) is used to retrieve monitoring data from the Trigger and Data Acquisition (TDAQ) [25] system and temporarily stores monitoring data in the form of status flags and counters to be shared between online applications. Histograms created by GNAM, as well as the monitoring histograms and results from the DQMF, are also sent to IS and can be retrieved [26, 27] to be rendered by dedicated monitoring display tools. The monitoring display tools provide an interface for the crew of *shifters*, who are at work in the ATLAS control room 24 hours a day,[5] to monitor data-taking in real time. Should these online systems indicate an issue with the trigger or a particular detector subsystem, experts are on call to resolve problems that concern their system to minimise the impact on the quality of ATLAS data.

The two major monitoring display tools that are used online in the control room are the Data Quality Monitoring Display (DQMD) [28] and the Online Histogram Presenter (OHP) [29]. The DQMD uses the results from the DQMF and presents them in a hierarchical manner, along with the corresponding monitoring histograms and details of the associated DQMF checks. This provides a global view of the detector status, with coloured status flags indicating the quality of the data according to the DQMF results. The OHP is a highly configurable histogram presenter, which can be used to display a large number of histograms to be monitored by subsystem, trigger, or DQ experts. The OHP permits the display of any published histogram in an arbitrary manner, while DQMD strictly visualises the histograms used by the DQMF in a hierarchical structure. All monitoring information is archived [30] such that status flags and other information can be propagated offline for DQ documentation.

ATLAS data that pass trigger requirements are organised into *streams*, where a stream is defined as a set of trigger selections and prescales and contains all events that have been stored to disk after satisfying any of those selections. This streaming is inclusive,[6] such that a single event can be included in multiple streams should it satisfy the corresponding selection criteria. Some streams exist for specific calibration purposes (e.g. electronic noise monitoring [31], beam-spot position [32], detector alignment [33]), while others are dedicated to collecting potentially interesting data for physics analysis. The *Express* stream contains a representative subset of the data collected in the physics and calibration streams,[7] and is promptly reconstructed at the ATLAS Tier 0 computing facility alongside most calibration streams. As reconstruction of these streams begins in parallel with data-taking, the data can be made available for offline DQ validation as quickly as possible, with monitoring histograms produced during the reconstruction process subsequently being analysed by the offline DQMF.

The DQ operational workflow is illustrated schematically in Figure 2. First, data are monitored online in real time using tools such as DQMD and OHP to display information to monitoring experts ("online shifters" in Figure 2) and alert them to the presence of issues. This first stage seeks to minimise data losses during data-taking, and is discussed in more detail in Section 4.2. Once the data have been recorded and reconstructed, a two-stage offline DQ assessment ensues. The first-pass assessment makes use of the

[5] Each 24 hour period is split into three control room shift blocks with an eight hour rotation.

[6] The exception to this inclusive streaming is the *Debug* stream, which contains events that have passed the L1 trigger, but encounter errors at HLT or DAQ level. This ensures that data encountering problems in the TDAQ system can be recovered. Events collected in this stream are not available in any other stream. Events entering the Debug stream constituted a fraction of less than 10^{-7} of the recorded dataset between 2015 and 2018, though physics analyses are asked to consider this stream to avoid missing potentially interesting events.

[7] The *Express* stream contains a minimal rate (~20 Hz) of events as required to perform a reliable first-validation of the detector subsystems and reconstructed physics objects.

promptly reconstructed subset of data from the Express and calibration streams (as illustrated by the orange and green boxes in Figure 2).

Based on this first look at the monitoring output of the data reconstructed offline, updates can be made to the conditions database by system DQ experts (as indicated by the arrows pointing to the conditions database in Figure 2), to be taken into account in the next stage of data processing. The implementation of these updates, and the procedures followed to ensure their validity, are described in detail in Section 4.3. Upon completion of this first iteration of checks, all streams, including the physics streams, are reconstructed (as shown in the "bulk data processing" box in Figure 2), making use of the new information gleaned from the first-pass DQ assessment. Once this full processing is complete a thorough assessment is made using the full data statistics available in the physics streams. The outcome of this iteration of DQ checks forms the basis for the decision as to which data are usable for physics analysis, and which must be discarded. A detailed walkthrough of this workflow is provided in Section 4, where both online monitoring (Section 4.2) and offline DQ assessment (Section 4.3) are discussed.

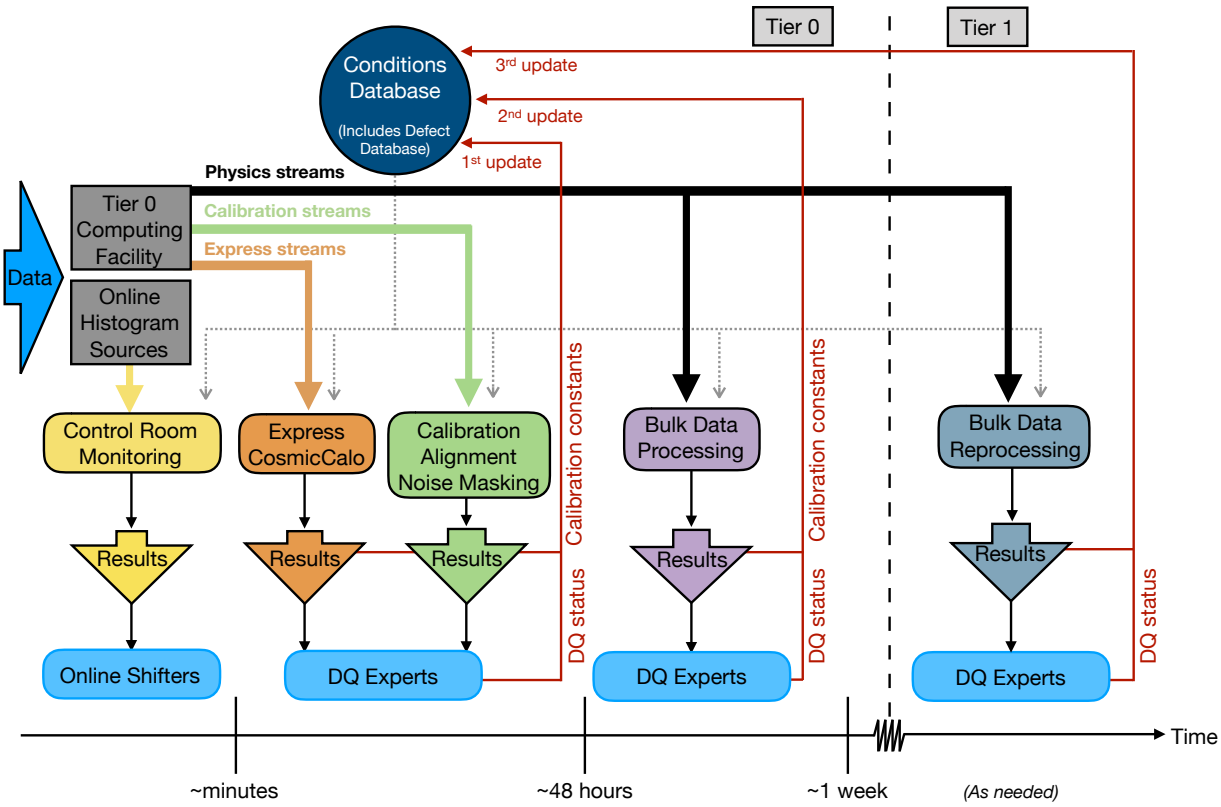


Figure 2: Schematic diagram illustrating the nominal Run 2 operations workflow for the data quality assessment of ATLAS data. Online histogram sources include the high-level trigger farm, the data acquisition system, and full reconstruction of a fraction of events accepted by the trigger.

The task of assessing the monitoring data associated with all detector components, and subsequent reconstructed objects, is shared among detector, trigger, and combined performance specialists, who constitute the "DQ Experts" indicated in Figure 2. While the detector specialists provide system-specific expertise, the combined performance assessment is split between several subgroups. The ID Global

group validates the combined performance of the ID subsystems and track reconstruction. A combined calorimeter objects group provides monitoring of reconstructed electrons, photons, τ-leptons, jets, and missing transverse momentum. Muon combined performance is monitored alongside the muon subsystems within the muon detector group. A dedicated *b-tagging* group is responsible for overseeing the DQ assessment of jets identified as containing b-hadrons. In the case of the trigger group, DQ assessment responsibilities are divided internally among several combined performance subgroups. Each of these is responsible for monitoring triggers that select specific physics objects or event-level quantities. The internal structure of the trigger group is similar to that of the central combined performance monitoring groups. The trigger and detector subsystems have dedicated shifters performing online monitoring in the ATLAS control room, in addition to the central online DQ shifter. For example, the ID shifter, responsible for monitoring the ID subsystems, has experience with the ID-specific hardware and software, and can provide more expert input should an issue arise. In the case of such an issue, all trigger and detector subsystems have dedicated on-call experts available to aid the control room shifters. Online monitoring of combined performance objects is, for the most part, performed by the online DQ shifter. There are exceptions to this. For example, owing to the large overlap between muon subsystem and muon reconstruction monitoring, the online muon shifter is responsible for the surveillance of muon object performance in addition to detector monitoring.

4 Data quality monitoring and assessment

The final product resulting from the DQ monitoring and assessment of ATLAS data is the so-called *Good Runs List* (GRL), a set of XML [34] files that contain the list of LBs that are certified for use in physics analyses for given runs taken over a given time period. These files are used to filter out data compromised by anomalous conditions, and are fully integrated into the analysis tools used by the ATLAS Collaboration. The integrated luminosity of a physics dataset, the so-called "good for physics" integrated luminosity, is calculated from the LBs that are included in these files. A GRL is created by querying the DQ status of the data at any given time using the ATLAS defect database [35]. The mechanism for recording this information in the database is described in Section 4.1, and the procedures followed to assess the DQ status of the data are detailed in Section 4.3.

4.1 Data quality defects

Data quality conditions are recorded by the setting of *defects* in the defect database, a subcomponent of the conditions database. A defect is set to denote an IOV (at LB-level granularity) where detector conditions are not nominal. It does not necessarily follow that data need be rejected as a consequence of a defect having been set. Although serious defects will result in data loss, a defect can also be set as an issue-tracking measure to ease data review in the future. Defects are stored in versioned COOL tags. The versioning mechanism both ensures the reproducibility of results and provides flexibility for defects to evolve over time. The latter can happen as DQ-related issues are addressed or the understanding of a detector problem is improved.

There are two different types of versioned defects. The *primary defects* are usually set manually by DQ and subsystem experts as a consequence of the assessment procedures that are described in Section 4.3. In some cases, primary defects are uploaded automatically, based on information from the DCS, for example. Primary defects are either *present* or *absent* for a given IOV, with the default state being absent unless

the defect is uploaded during the DQ review. These primary defect values are associated with a specific iteration of the data processing, such that they are linked to a time period with uniform conditions. The *virtual defects* define the logic that is used to determine whether or not the presence of a primary defect can be tolerated, or if it is necessary to reject data from analysis as a consequence of that defect having been set. Virtual defects are defined by a logical combination of primary defects or other virtual defects. In contrast to primary defects, virtual defects are not stored in the database, but are computed upon access. The virtual defect definitions tend to evolve more slowly than the values of the primary defects. For example, all LAr calorimeter system defects that are serious enough to warrant the rejection of data from physics use are used to define a single LAr calorimeter virtual defect. If any one of these serious LAr defects is set for a given IOV, the corresponding LAr virtual defect is also set by definition, as detailed in Ref. [35]. In this way the virtual defect contains the information referencing which primary defects describe conditions where the corresponding data should not be used. This simplifies the process of querying the defect database when creating a GRL.

For automatic defect assignments, data from the DCS archive are used as input to a DCS defect calculator program, which interprets DCS information to assign defects that indicate suboptimal status of the detector hardware. For example, the values of the ATLAS solenoid and toroid magnet currents are continuously sampled and stored in the DCS archive. Should these currents be below a nominal threshold a primary defect is automatically uploaded to the defect database by the DCS defect calculator to indicate that the magnets are not at nominal magnetic field. The corresponding IOV for which this defect is present denotes the period of time for which the magnet currents are found to be below threshold. Similar checks exist for the detector subsystems, such as the ID and MS, which ramp up only after the LHC has declared stable beam conditions. In order to establish whether, for example, the RPC subsystem has reached nominal HV status and is therefore ready for physics data, the number of RPC HV channels that have reached the desired voltage is monitored by the DCS calculator, using information from the DCS archive. Once this number exceeds a predefined threshold the HV ramp up can be deemed "complete" for the RPC subsystem. Until then, from the point at which the LHC declares stable beams, the DCS calculator will automatically set a defect to document that data collected during this time period have been taken while the RPCs were still ramping up.

In general, a single primary defect is defined so as to be applicable to a given type of issue that can occur during data-taking. In the case of the RPC subsystem example above, a specific defect exists to document that the RPC system is still in the process of ramping up to become ready for data-taking. The meaning of the defect and the class of situations to which it is applicable is documented in the defect database for each defect by way of a *description* field. Metadata accompany each entry made to the defect database. This includes an entry timestamp, the identification of the person or process that uploaded the defect itself, and a comment input by the uploader to add auxiliary information as to the particular issue or occurrence that necessitates the defect upload. In Run 2 there were a total of ~450 different primary defects defined that could be used to track DQ issues with ATLAS data.

4.2 Online data quality monitoring

Data quality monitoring begins in real time in the ATLAS control room. Online shifters on duty serve as a first line of defence to identify serious detector-related issues. Should an issue occur that requires an intervention during data-taking it is important that it is identified quickly to minimise data loss.

Monitoring information stored in the IS can be retrieved to allow DQ monitoring at various levels of the ATLAS data-flow. The subset of Express stream data reconstructed online is quickly made available to the online shifters via the display tools described in Section 3. The DQMF tests performed on the reconstruction output can include compatibility checks between the observed distributions from the monitoring data and so-called *reference* histograms, which are corresponding monitoring histograms taken from a past run that is both free of DQ issues and taken with similar machine operating conditions. Other tests might involve checks on the number of bins in a histogram above a predefined threshold, or checks on the gradient of a distribution. For example, histograms that monitor read-out errors should always be empty under "ideal" conditions. If a bin in such a histogram has a non-zero number of entries, a flag would be raised to alert the shifter to the problem. Online event reconstruction also allows control room DQ shifters to monitor reconstructed physics objects, such as electrons or ID tracks, permitting real-time monitoring of combined performance in addition to detector status. For example, if the hit occupancy per unit area in the Pixel, SCT and TRT subsystems is uniform, but a hole or "cold spot" is visible in histograms that monitor track occupancy, this could point to a localised calibration issue that may be difficult to spot using individual subsystem monitoring alone. The DQMF takes the results of tests on individual histograms and propagates them upwards through a tree, resulting in a set of top-level status flags, which can be viewed on the DQMD, that alert shifters to potential problems in various subdetectors. Monitoring histograms are updated to include additional data every few minutes as newly available data are reconstructed. In this way, online monitoring allows hardware- or software-related issues to be caught in real time and rectified so as to minimise the impact on collected data.

4.3 Data quality assessment

Daily notification emails are distributed to offline data quality shifters, containing information about the current processing status of recent ATLAS runs. This includes details of which runs are ready for DQ assessment. The subsequent two-stage assessment workflow follows that introduced in Section 3 and illustrated in Figure 2.

Once a run has come to an end and the prompt reconstruction of the Express and calibration streams is complete, the offline DQ assessment begins. The DQMF extracts information from the reconstruction monitoring output in the form of status flags or numerical results. These monitoring and reference histograms, as well as the results from the DQMF, are transferred to the offline DQ server, a virtual machine upon which all subsequent offline DQ operational and assessment procedures take place.

Once on the DQ server, the results of the DQMF checks are displayed – including the output histograms on which the DQMF algorithms are run – on dedicated, centrally provided web pages that can be accessed outside of the CERN network. The web pages are used by detector system, trigger, and combined performance experts to access monitoring information. Experts can navigate the web pages to view the monitoring histograms for their respective area. In cases where status flags have been assigned as a consequence of the data quality checks performed by the DQMF, these are shown alongside the various histograms. These flags operate under a traffic-light system, with red indicating a potential issue, yellow proposing a manual review of the distribution in question, and green signalling that the respective automatic checks were passed. Where relevant, the data of the monitored run are overlaid with data from the assigned reference run. There is also a mechanism to allow experts to view the same monitoring output from different runs side by side for further comparisons or for investigative purposes. Comparing the data with reference distributions forms an important part of the validation.

Data quality checks on the Express stream data allow for early scrutiny of a subset of the data collected during a given run, making it possible to act to correct DQ issues that might be mitigated during data reconstruction. Should this be the case, by updating calibration constants for example, changes to the conditions can be implemented prior to the physics streams being processed. This constitutes the first update to the conditions database, as illustrated in Figure 2. At this stage, conditions updates ensure that data can still be cleaned, or rejected, at a granularity far finer than a luminosity block.

Detector experts use the calibration streams to verify the conditions for detector subsystems, updating calibration constants and detector alignment information in the conditions database as necessary. The *SCTNoise* calibration stream contains only events in bunch crossings where the bunches are not filled with protons (so-called *empty* bunch crossings). Negligible collision activity is expected in these bunch crossings. Data from this stream are used to identify noisy SCT strips. Having been identified in this stream, which contains a noise-dominated data sample, these strips can then be masked in the software to prevent noise in the SCT system from biasing track reconstruction.[8] Events in the *CosmicCalo* stream are selected on the basis of low-threshold calorimeter activity occurring in empty bunch crossings, providing a sample enriched with electronic noise from the calorimeter [31]. These data are used alongside dedicated calorimeter calibration streams[9] to identify noisy channels that must be masked in reconstruction,[10] and to diagnose bursts of noise originating in the calorimeter that must be rejected from physics analyses in a procedure detailed in Ref. [31]. In the latter case, the timestamp at which the burst occurs is identified and all data collected within a window of $\mathcal{O}$(ms) surrounding that timestamp is marked as being within a noise burst IOV. By uploading these time windows to the conditions database, the corresponding data can be marked during the imminent reconstruction of the physics streams so that they can be rejected in physics analyses. This same procedure is used in order to reject small time windows where data from the LAr system are corrupted. To account for the impact of rejecting these small time windows from the dataset, these IOVs are removed when calculating the total "good for physics" integrated luminosity of the corresponding dataset. The data rejected during these time windows are consequently accounted for in the total DQ inefficiency. Approximately 69 pb^{-1} of data were rejected from the standard $\sqrt{s}$ = 13 TeV dataset as a consequence of rejecting time windows over the course of Run 2.

The conditions to be updated during this first-pass assessment of the offline-reconstructed data also include constants pertaining to the alignment of the ID subsystems [33],[11] and the precise determination of the "beam spot" location [32], the luminosity-weighted centroid of which defines the average collision point. The LAr, SCT, beam spot, and alignment folders in the conditions database must be updated with the relevant information before the bulk reconstruction of all physics streams is launched.

This process of database updates and primary DQ review is known as the *calibration loop*. The calibration loop typically lasts ~48 hours from the point at which the first-pass data processing begins, although this can be further shortened to 24 hours during busy periods. In exceptional cases the calibration loop can be

[8] The masking of an SCT strip results in the strip being ignored in the track reconstruction.

[9] The *LArCellsEmpty* stream contains "partially built" events from empty bunch-crossings, where only the LAr cells associated with a high-energy deposit are stored. This results in a reduced event size, permitting both the use of lower energy thresholds for the events to be recorded and larger samples to be stored. The *LArNoiseBurst* stream contains noise burst candidate events, which are identified (and their timestamps marked) at the HLT-level. This early identification, a significant improvement relative to pre-2015 operations, facilitates noise burst rejection during these first DQ checks, yielding a cleaner sample in which to study and identify noisy channels.

[10] The masking of a LAr channel results in the energy deposited in that channel being ignored, with the corresponding cell energy instead being estimated from the average energy of the eight neighbouring channels within the same calorimeter layer.

[11] The dedicated *IDTracks* stream is used to obtain a precise determination of the positions of the sensitive ID elements and their geometrical distortions relative to the ideal or designed geometry.

delayed at the request of detector subsystem experts, effectively putting full reconstruction on hold until the issue prompting the delay is resolved. Such situations are rare, but can arise due to problematic database uploads, excessive detector noise requiring further investigation, or reconstruction failures.

Once the database conditions are up to date and the calibration loop delay expires, processing of the physics streams is launched, taking into account these updated conditions. The reconstructed dataset is usually available after 24–48 hrs, at which stage a final DQ assessment is performed on the full data statistics. Detector system and combined performance experts scrutinise the monitoring output once more, either using the dedicated web-page displays or running stand-alone algorithms directly on the monitoring output. At this stage it is important not only to validate the quality of the full dataset, but also to ensure that conditions updates during the calibration loop have been applied successfully. For example, Figure 3 shows the transverse-plane distance of closest approach of charged-particle tracks to the beamline (the *transverse impact parameter*, d_0) versus ϕ before and after the beam-spot determination during the calibration loop. Following the calibration loop, where updated beam-spot conditions are applied, the distribution should be flat, as illustrated in the right panel of Figure 3.

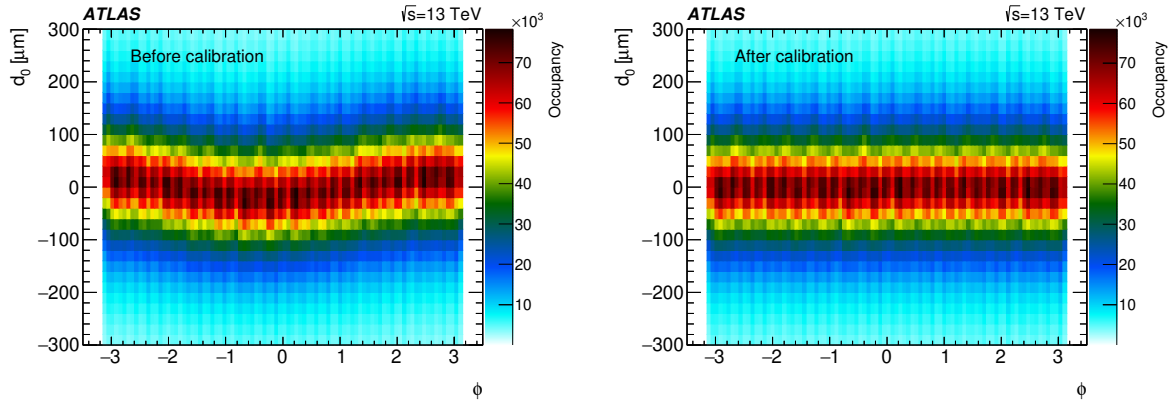


Figure 3: Transverse impact parameter d_0 versus ϕ for charged-particle tracks. Left: For the first processing of the Express stream, the beam-spot location is not yet known accurately and d_0 is calculated relative to the beam-spot position as determined online. Right: A correctly determined beam spot results in a flat distribution after the application of updated conditions during the calibration loop, since here d_0 is calculated relative to the reconstructed beam spot.

With the full reconstruction complete, any remaining issues that act to the detriment of the DQ at this stage, such as residual noise or non-negligible losses in coverage, are documented by assigning an appropriate defect to the affected IOV, at luminosity block granularity, in the defect database.

A second update to the conditions database is possible at this stage to provide more complete rejection of LAr noise, for example. This further update to the conditions would only be applied should the data be subject to a reprocessing, i.e. rerunning the reconstruction procedure with an updated configuration. For the LAr noise example, a conditions update may facilitate a more thorough cleaning of LAr noise using finer-granularity time windows. In such a case, previously set LAr noise primary defects may be removed from the corresponding LBs as a consequence of this more granular cleaning. This is an example of a primary defect evolving with a new iteration of the data processing. The implication here is that data reprocessing campaigns can result in improved DQ efficiency for a given dataset. Reprocessing campaigns can take place as needed, but large-scale reprocessings will generally occur once a year at most to incorporate final conditions and any important software improvements. This brings the reconstruction configuration for a large dataset collected over a long period of time into alignment. By this stage the

data will have been distributed to Tier 1 sites, as indicated on the far right of Figure 2, and so further data reprocessings do not take place at the Tier 0 computing facility.[12] Any time that the data are reprocessed the DQ validation procedure is repeated to rule out the presence of any insidious effects resulting from the updated conditions or reconstruction software. Both the output histograms and the results from DQMF are archived for future reference, as is the case for every data processing iteration. This information, used for the DQ web pages through which a large portion of the offline DQ assessment is performed, is stored in a ROOT [36] file format. These files, for data taken in 2015–2018, including the first-pass processing, bulk data processing, and bulk data reprocessing campaigns, amount to a total of approximately 10 TB of data. During a single processing of the main physics stream for a single ATLAS run $\mathcal{O}(100\text{k})$ monitoring histograms are produced. While it is important that monitoring information is available in order to quickly study DQ issues, the number of histograms and their respective granularities are constantly reviewed to minimise the impact on processing time and storage resources.

Table 2: Summary of the data quality groups involved in the continuous review and sign-off of ATLAS data. Included are details pertaining to the nominal shift crew responsible for DQ assessment in each area. If a dedicated online shifter is responsible for the online monitoring of a system in addition to the online DQ shifter, this is indicated under the "dedicated control room shifter" column. Should a subsystem or group be responsible for routinely updating DQ-related conditions during the calibration loop, this is indicated under "conditions updates", with the corresponding streams monitored for DQ purposes during the calibration loop listed in the neighbouring column. If any of the defects under the responsibility of a given group are uploaded automatically this is indicated in the last column.

Group/Subsystem	Dedicated Control Room Shifter	Offline DQ Shifters & Experts	Conditions Updates (calibration loop)	Calibration Loop Streams	Automatic Defect Assignment
Pixel	ID shifter	1 shifter 1 expert	Disabled module masks	Express	Yes
SCT		1 shifter 1 expert	Noisy strip masks	SCTNoise Express	Yes
TRT		1 shifter 2 experts	Dead straws	Express	No
LAr	Calorimeter shifter	2 shifters 2 experts	Noisy channel masks Noise burst rejection Data corruption	LArCellsEmpty LArNoiseBurst CosmicCalo Express	No
Tile		1 shifter 1 expert	–	Express	Yes
L1	Trigger shifter	1 shifter 1 expert	–	Express	No
HLT		1 shifter 5 experts	–	Express	Yes
b-tagging	–	1 shifter 2 experts	–	Express	No
Calorimeter objects	–	1 shifter 5 experts	–	Express	No
ID Global	–	1 shifter 2 experts	ID alignment Beam-spot position	IDTracks BeamSpot Express	Yes
Muons (subsystem & performance)	Muon shifter	1 shifter 1 expert	–	Express	Yes
Luminosity	–	1 shifter 1 expert	–	Express	Yes

An overview of the DQ monitoring groups and their organisation, introduced in Section 3, is given in

[12] Though data reprocessings are nominally performed at Tier 1 sites to ensure that Tier 0 resources are available for prompt data reconstruction, the Tier 0 can be seamlessly included as an additional ATLAS WLCG site when it is not otherwise in use.

Table 2. Offline DQ assessment typically involves at least one offline shifter and one longer-term expert per subsystem or combined performance area. As shown in Table 2, in some cases the complexity of the assessment procedure requires larger teams. For example, the trigger DQ assessment requires input from several physics signature experts; and the nature and multiplicity of the LAr calibration loop updates requires that the work be shared between two shifters. In addition to the calibration loop updates already discussed, both the pixel and TRT subsystems must update the database with information about any newly disabled pixel modules or TRT straws, such that no activity should be expected in these regions during reconstruction. Conditions updates from other subsystems are also possible during the calibration loop, although they do not form part of the routine DQ workflow carried out for every ATLAS physics run. Subsystem and trigger DQ experts and shifters frequently interact with the ATLAS experiment operations teams. This ensures efficient communication of matters that may influence decisions related to DQ. Usually it is the DQ experts who take responsibility for uploading defects to the defect database, based on the initial DQ assessment carried out by the offline DQ shifters. While some subsystems make use of the automatic defect upload facility (by using the DCS calculator for example), combined performance groups do not. The only exception to this is for beam-spot monitoring; in cases where an accurate determination of the beam-spot position has not been possible, the corresponding IOV is automatically marked to flag this. Otherwise, automatic defects primarily mark data affected by detector hardware problems, or periods of time during which a particular detector element is not operational.

The full data validation procedure is overseen by ATLAS data quality and data preparation coordination, with formal sign-off of the data taking place on a weekly basis during dedicated meetings. The validation of the full dataset involves the collaboration of detector, trigger, and physics object reconstruction and performance experts. Typically, new runs can be fully validated 1–2 weeks after having been delivered by the LHC.

Once a given portion of runs have completed DQ validation (for example, at the close of a data-taking *period*)[13] a new GRL can be generated and propagated to physics analysis groups so that they can select appropriate data for analysis. The GRL is generated by querying the defect database for a selection of runs and LBs that satisfy predefined "good for physics" conditions. The "good for physics" definition is itself contained in a virtual defect, and so the criteria used to determine whether data enter a GRL are documented in versioned COOL tags. Safety defects exist to ensure that runs that have not been validated do not enter the GRL. For example, each run initially has a so-called `NOTCONSIDERED`[14] defect assigned for all LBs until it is released to DQ experts for assessment. For each run taken outside normal data-taking periods, where the data are not meant for physics use in analyses, the `NOTCONSIDERED` defect remains in place such that it is not propagated to DQ experts. Furthermore, each detector system and physics object group that scrutinises the data in the procedure described in this section must manually remove a so-called `UNCHECKED` defect from the database for each run once their validation is completed. A GRL cannot be generated while an `UNCHECKED` defect remains present for any of the data being considered.

There are cases where special GRLs are made available to analysers, where the standard "good for physics" definition may not be suitable, or a significant fraction of the recorded data is rejected owing to a defect that can be tolerated by a specific analysis. For example, physics analyses that do not rely on muon identification may be able to use data taken during periods where the ATLAS toroids were not operational. In such a case a special GRL can be made that includes data that would otherwise be rejected owing to magnet defects.

[13] Runs are grouped together into *periods* during which data-taking conditions are considered to be uniform.
[14] Data marked with a `NOTCONSIDERED` defect would not be permissible in physics analyses.

5 Data quality performance

Detector-, trigger-, reconstruction-, or processing-related problems that result in data being rejected on the grounds of DQ are accounted for in the DQ efficiency. The DQ efficiency is calculated relative to recorded, rather than delivered, integrated luminosity. In some cases, detector-related processes or problems result in data not being recorded for physics by ATLAS in the first place. This includes data taken during the so-called "warm start" that the tracking detectors undergo once the LHC declares "stable beams", which involves ramping up the high voltage and turning on the preamplifiers for the pixel system. The inefficiency due to the time it takes for the pixel preamplifiers to turn on is included in the ATLAS data-taking efficiency. This is defined as the fraction of data delivered by the LHC recorded by ATLAS, regardless of the quality of the data. Should remaining detector subsystems still be undergoing high-voltage ramp up after the warm start is complete, the inefficiency due to this is accounted for in the DQ efficiency.

The data quality efficiency is presented in terms of a luminosity-weighted fraction of good quality data recorded during stable beam periods. Only periods during which the recorded data were intended to be used for physics analysis are considered for the DQ efficiency. In particular, this excludes machine commissioning periods, special runs for detector calibration, LHC fills with a low number of circulating bunches or bunch spacing greater than 25 ns, and periods before beams were separated to achieve low-μ conditions for low-μ runs.[15] The defect database framework allows defects to be associated with a given detector subsystem, reconstruction algorithm, or operating condition. DQ defects can be associated with physics objects as well, but in these cases there is generally some underlying detector-level cause behind the issue. It is therefore possible to express the DQ efficiency during Run 2 data-taking in the context of each detector subsystem, and to present an overall DQ efficiency for ATLAS during Run 2.

The luminosity-weighted fraction of good quality data delivered during stable beam periods for 2015, 2016, 2017, and 2018 is presented in Tables 3, 4, 5, and 6, respectively. Since the presented efficiencies are weighted according to integrated luminosity the efficiency is dominated by periods of standard pp data-taking at $\sqrt{s} = 13$ TeV. The DQ efficiencies for data-taking campaigns using other machine configurations, as detailed in Table 1 (including $\mu = 2$ pp data taken at $\sqrt{s} = 13$ TeV), are displayed separately in these tables. The total DQ efficiency improved over the course of Run 2, with 88.8% in 2015, 93.1% in 2016, 95.7% in 2017 and 97.5% in 2018, for the (dominant) standard $\sqrt{s} = 13$ TeV pp data-taking campaigns of each year. Combining these efficiencies results in a total data quality efficiency of 95.6% for the standard Run 2 $\sqrt{s} = 13$ TeV pp dataset, with a corresponding 139 fb^{-1} of data certified as being good for physics analysis. The DQ-related inefficiencies per subsystem corresponding to this dataset are illustrated in Figure 4 and presented in Table 7, and the cumulative "good for physics" integrated luminosity versus month in a year is shown alongside the corresponding delivered and recorded integrated luminosities in the top panel of Figure 5. The evolution of the DQ efficiency as a function of collected integrated luminosity is illustrated in the bottom panel of Figure 5, where the more significant DQ-loss incidents can be seen as sharp drops in the cumulative DQ efficiency. For example, the sharp decline from ~98% to 94% around the 10 fb^{-1} mark in 2017 is due to three runs where the ATLAS toroids were not operational.

Periods during which the toroids are not in operation are typically not used for physics analysis,[16] although these data are useful for alignment of the muon system, making these periods profitable despite the associated inefficiency indicated in Table 7. These data can also be used for other detector-related studies

[15] In order to achieve low-μ conditions the LHC begins colliding the beams head-on, before slowly separating them in the transverse plane to reduce the average number of interactions per bunch crossing.

[16] There is an exception to this for analyses that do not rely on muon reconstruction [37–39].

or for calibration purposes, and in these cases the subsystem in question often switches into a non-standard data-taking configuration to facilitate online tests. The DQ efficiency for the subsystem in question is not impacted as a result of being in a non-standard configuration in these cases, since these periods occur in the "shadow" of a magnet issue and hence are accounted for in the inefficiency quoted for the toroids and/or solenoid. The same accounting principle is applied in cases where a specific detector subsystem is switched off, for example. Should other subsystems take advantage of this to perform studies specific to their subsystem, the corresponding DQ inefficiency is assigned only to the subsystem that is off.

Table 3: Luminosity-weighted relative detector uptime and good data quality efficiencies (in %) during stable beams pp collision physics runs at $\sqrt{s}$ = 13 TeV and 5.02 TeV between July and November 2015. Also shown are 0.49 nb^{-1} of Pb-Pb collision data collected at $\sqrt{s_{NN}}$ = 5.02 TeV between November and December 2015.

2015 Data Quality Efficiency [%]													
Dataset	Inner Tracker			Calorimeters		Muon Spectrometer				Magnets		Trigger	
	Pixel	SCT	TRT	LAr	Tile	MDT	RPC	CSC	TGC	Solenoid	Toroid	L1	HLT
pp @ 13 TeV (50 ns)	99.84	99.63	95.28	98.53	100	95.28	100	100	99.70	100	95.87	100	99.94
pp @ 13 TeV	93.84	99.77	98.29	99.54	100	100	99.96	100	99.97	100	97.79	99.97	99.76
pp @ 5.02 TeV	100	100	100	100	100	100	99.96	100	99.94	100	100	99.24	100
Pb-Pb @ 5.02 TeV	100	100	99.64	97.57	100	99.80	99.98	99.90	99.89	100	100	100	100

		Data Quality Efficiency [%]	Integrated Luminosity
pp @ 13 TeV (50 ns)	Good for Physics	88.77	83.9 pb^{-1}
pp @ 13 TeV		88.79	3.22 fb^{-1}
pp @ 5.02 TeV		99.14	25.3 pb^{-1}
Pb-Pb @ 5.02 TeV		96.76	0.49 nb^{-1}

Table 4: Luminosity-weighted relative detector uptime and good data quality efficiencies (in %) during stable beams in pp collision physics runs at $\sqrt{s}$ = 13 TeV between April and October 2016. Also shown is 165 nb^{-1} of p-Pb collision data collected at $\sqrt{s_{NN}}$ = 5.02 and 8.16 TeV between November and December 2016.

2016 Data Quality Efficiency [%]													
Dataset	Inner Tracker			Calorimeters		Muon Spectrometer				Magnets		Trigger	
	Pixel	SCT	TRT	LAr	Tile	MDT	RPC	CSC	TGC	Solenoid	Toroid	L1	HLT
pp @ 13 TeV	98.98	99.89	99.74	99.32	99.31	99.95	99.80	100	99.96	99.15	97.23	98.33	100
p-Pb @ 8.16 TeV	99.92	100	100	100	99.99	100	99.94	100	100	100	100	100	100
p-Pb @ 5.02 TeV	100	99.96	100	100	100	100	99.96	100	99.95	100	100	100	90.44

		Data Quality Efficiency [%]	Integrated Luminosity
pp @ 13 TeV	Good for Physics	93.07	33.0 fb^{-1}
p-Pb @ 8.16 TeV		98.35	165 nb^{-1}
p-Pb @ 5.02 TeV		82.93	0.36 nb^{-1}

The detector subsystems, the L1 trigger, and the HLT achieved excellent DQ efficiencies during Run 2. While there typically exist known sources of low-level DQ-related data loss at the subsystem or trigger level throughout Run 2 data-taking, often the largest contributions to the DQ inefficiency come from one-off incidents. In the case of low-level recurring issues, improved understanding and continuous infrastructure development can mitigate the impact of these sources of DQ losses over time. For single incidents that result in more-significant DQ losses, lessons must be learned and countermeasures put in place to minimise the risk of similar incidents occurring again. The main sources of DQ-related losses per subsystem are discussed in the following.

The pixel detector began operation in 2015 with the newly installed IBL. During 2015 data-taking, instabilities were observed from the CO_2 cooling required for IBL operation. In order to correct the issue it was necessary to take data with the IBL powered off so that the cooling parameters could be optimised. The 0.2 fb^{-1} of data rejected during this time as a consequence of operating without the IBL constitutes a DQ inefficiency of 6%, making up the largest single contribution to the DQ inefficiency for 2015 (see

Table 5: Luminosity-weighted relative detector uptime and good data quality efficiencies (in %) during stable beams in pp collision physics runs at $\sqrt{s}$ = 13 TeV between June and November 2017, including 147 pb^{-1} of good pp data taken at an average pile-up of $\mu = 2$. Online luminosity errors, which are not displayed separately in this table, contribute 0.48% to the total $\sqrt{s}$ = 13 TeV pp DQ inefficiency. Also shown are 257 pb^{-1} of good pp data taken at $\sqrt{s}$ = 5.02 TeV in November and 1.96 nb^{-1} of Xe-Xe collision data taken at $\sqrt{s_{NN}}$ = 5.44 TeV in October.

2017 Data Quality Efficiency [%]													
Dataset	Inner Tracker			Calorimeters		Muon Spectrometer				Magnets		Trigger	
	Pixel	SCT	TRT	LAr	Tile	MDT	RPC	CSC	TGC	Solenoid	Toroid	L1	HLT
pp @ 13 TeV	99.97	99.94	99.32	99.48	99.41	99.90	99.24	99.89	99.98	100	99.17	99.95	99.96
Xe-Xe @ 5.44 TeV	100	100	100	99.98	100	100	100	100	100	100	100	100	100
pp @ 5.02 TeV	100	99.73	100	99.96	99.99	95.42	99.98	100	99.99	100	100	100	100
pp @ 13 TeV ($\mu = 2$)	100	100	100	100	100	99.49	100	100	100	100	100	100	100

		Data Quality Efficiency [%]	Integrated Luminosity
pp @ 13 TeV	Good for Physics	95.67	44.39 fb^{-1}
Xe-Xe @ 5.44 TeV		99.98	1.96 nb^{-1}
pp @ 5.02 TeV		95.20	257 pb^{-1}
pp @ 13 TeV ($\mu = 2$)		99.28	147 pb^{-1}

Table 6: Luminosity-weighted relative detector uptime and good data quality efficiencies (in %) during stable beams in pp collision physics runs at $\sqrt{s}$ = 13 TeV between April and October 2018, including 193 pb^{-1} of good data taken at an average pile-up of $\mu = 2$. Dedicated luminosity calibration activities during LHC fills used 0.64% of the recorded data (including ~4% of the $\mu = 2$ dataset) and are included in the inefficiency. Also shown are 1.44 nb^{-1} of good Pb-Pb collision data taken at $\sqrt{s_{NN}}$ = 5.02 TeV between November and December.

2018 Data Quality Efficiency [%]													
Dataset	Inner Tracker			Calorimeters		Muon Spectrometer				Magnets		Trigger	
	Pixel	SCT	TRT	LAr	Tile	MDT	RPC	CSC	TGC	Solenoid	Toroid	L1	HLT
pp @ 13 TeV	99.78	99.77	100	99.67	100	99.80	99.72	99.98	99.98	100	99.58	99.99	99.99
pp @ 13 TeV ($\mu = 2$)	100	100	100	100	100	99.07	99.94	100	99.98	100	100	98.03	100
Pb-Pb @ 5.02 TeV	100	100	100	99.99	100	100	100	100	99.98	100	83.25	99.97	100

		Data Quality Efficiency [%]	Integrated Luminosity
pp @ 13 TeV	Good for Physics	97.46	58.5 fb^{-1}
pp @ 13 TeV ($\mu = 2$)		92.86	193 pb^{-1}
Pb-Pb @ 5.02 TeV		82.54	1.44 nb^{-1}

Table 3). Desynchronisation of data read-out from the pixel detector was a constant source of DQ-related losses in 2015–2017, but the situation improved over the course of data-taking as a result of continuous firmware and software development, and the replacement of the read-out hardware.

Problems related to read-out in the SCT resulted in DQ inefficiencies at the sub-percent level during 2015. Improvements in the read-out firmware at the end of 2015 resolved this issue, with SCT read-out problems having negligible impact on DQ in the subsequent years. The largest DQ-related loss for the SCT occurred as a result of a one-time online-software problem during 2018, with ~130 pb^{-1} of $\sqrt{s}$ = 13 TeV pp data affected. The software problem caused an immediate halt to SCT clustering, preventing the reconstruction of ID tracks. Online shifters in the control room identified the absence of tracks using the DQ monitoring displays, but it took two hours to locate the issue and apply a correction to the relevant software. Following the software fix, new monitoring histograms were added to the online monitoring displays to make it easier to quickly identify SCT issues specific to clustering and track reconstruction.

The lowest DQ efficiency quoted for the TRT subsystem during Run 2 is shown in Table 3 for the 2015 standard $\sqrt{s}$ = 13 TeV pp dataset, at 98.3%. At 1.4%, most of this inefficiency is due to a single event during November 2015, where a problematic database update resulted in incorrect latency settings for the TRT being loaded into the online database. Online monitoring histograms showing the number of TRT hits

Table 7: Luminosity-weighted relative detector uptime and good data quality efficiencies (in %) during stable beams in standard 25 ns pp collision physics runs at $\sqrt{s}$ = 13 TeV between July 2015 and October 2018. Dedicated luminosity calibration activities during LHC fills used 0.64% of the data recorded during 2018, and are included in the inefficiency. Online luminosity errors, which are not displayed separately in this table, are also included and contribute 0.15% to the total Run 2 DQ inefficiency.

Run 2 Data Quality Efficiency [%]													
Dataset	Inner Tracker			Calorimeters		Muon Spectrometer				Magnets		Trigger	
	Pixel	SCT	TRT	LAr	Tile	MDT	RPC	CSC	TGC	Solenoid	Toroid	L1	HLT
Standard pp @ 13 TeV	99.50	99.85	99.68	99.52	99.65	99.83	99.60	99.96	99.98	99.79	98.84	99.57	99.94

		Data Quality Efficiency [%]	Integrated Luminosity
Standard pp @ 13 TeV	Good for Physics	**95.60**	**139.04 fb^{-1}**

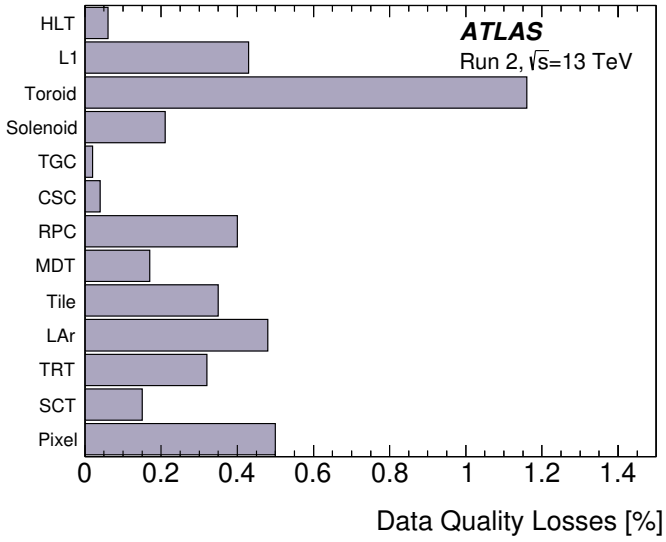


Figure 4: Luminosity-weighted data quality inefficiencies (in %) during stable beams in standard pp collision physics runs at $\sqrt{s}$ = 13 TeV between 2015 and 2018.

per track in the control room clearly conveyed that there was a TRT issue, with the shapes of the observed distributions differing significantly from the reference histograms. Following expert intervention the issue was resolved, with 50 pb^{-1} of data having been lost. Database update protocols for the TRT subsystem were improved as a consequence of this incident.

High-voltage trips were the major source of DQ losses for the LAr calorimeter system during 2015, contributing 0.2% to the total 0.5% DQ inefficiency quoted for the LAr system during standard $\sqrt{s}$ = 13 TeV pp data-taking in 2015. The subsequent replacement of problematic modules with more-robust current control modules at the end of 2015 reduced the impact of HV trips from 2016 onwards by over 90%. The largest DQ-related loss for both the LAr and Tile calorimeter subsystems during 2016 resulted from the same incident, described in the following. For a single run in 2016, a misconfiguration in the online database resulted in calorimeter cell noise thresholds being too low. This resulted in problems for the trigger, with too many clusters being created from the calorimeter, overloading the HLT computing farm. Following intervention by software experts, the situation was resolved but, in the meantime, emergency measures had to be put into effect by the trigger, making the data collected effectively unusable for physics

analyses. In total, ~140 pb^{-1} of pp data were rejected as a result of this issue, contributing 0.4% to both the total 0.7% LAr inefficiency and the total 0.7% Tile inefficiency during standard $\sqrt{s}$ = 13 TeV pp data-taking quoted for 2016 in Table 4. As a result of this incident, software was introduced to allow trigger experts to run tests after an update is made to the online database to validate the database configuration prior to the start of a new run. In addition, calorimeter cluster occupancy monitoring was improved, with dedicated histograms being introduced at the central DQ desk in the control room to be monitored by the DQ shifter. Hardware issues resulting in an intolerable loss of detector coverage also affected both the LAr and Tile calorimeter subsystems during 2017. At the end of August, ~120 pb^{-1} of data were lost when a water leak resulted in a power supply trip, disabling a quarter of the LAr barrel calorimeter. A hardware issue also resulted in half of the Tile barrel being disabled, with a subsequent data loss of 265 pb^{-1} of $\sqrt{s}$ = 13 TeV pp collision data. Following this incident the affected hardware was inspected and, where necessary, replaced, to avoid future occurrences of similar problems.

The muon system operated with excellent DQ performance during Run 2, with a DQ efficiency consistently at or above 99.8%. An exception to this was observed in 2017 for the RPC system, where a hardware problem resulted in an unacceptable coverage loss on both sides of the detector. The extent of the loss in coverage is shown in Figure 6, where the absence of hits being recorded in individual RPC sectors indicates the problem. The issue was identified in real time in the control room due to DCS alarms indicating that the RPC currents were not as expected, and a hardware intervention was necessary to replace a problematic HV crate. Given the impact of this loss in coverage for muon reconstruction, as shown in the bottom panel of Figure 6, this single event caused the rejection of ~500 pb^{-1} of pp collision data, resulting in a lower than usual DQ efficiency of 99.2% for the RPC subsystem in 2017.

The L1 and HLT trigger systems generally rely on information provided by detector subsystems, and therefore most trigger-related DQ issues can be traced to a detector problem further upstream. The trigger operated throughout Run 2 with very little DQ-related loss, as indicated in Table 7. During 2016, however, an L1 trigger hardware issue resulted in a mis-timing of muon and jet triggers over the course of four runs, affecting ~590 pb^{-1} of pp collision data. The resulting drop in DQ efficiency can be seen in Figure 5 as a sharp drop in the 2016 DQ efficiency at ~12 fb^{-1}. This is reflected in the L1 DQ efficiency of 98.3% for the $\sqrt{s}$ = 13 TeV pp collision dataset in 2016, as shown in Table 4.

Data taken during emittance scans are used for luminosity calibration purposes, but the non-standard vdM-like configuration is unsuitable for standard physics analyses. These data must therefore be rejected from physics analysis GRLs. Dedicated emittance scans for luminosity calibration taken during standard data-taking runs accounted for 0.64% of the total DQ inefficiency during 2018.

The beginning of Run 2 data-taking during 2015 involved commissioning new detector hardware such as the IBL, and required the careful monitoring of all ATLAS subsystems to understand any constraints or potential issues connected with operating under the more challenging machine conditions of Run 2. A high DQ efficiency was achieved as a consequence of continuous detector maintenance, software development and monitoring of DQ performance over the course of Run 2. As the underlying sources of DQ losses were identified and addressed, actions were taken to reduce the probability of subsequent occurrences. By learning from DQ-related issues in this way the overall ATLAS DQ efficiency during standard $\sqrt{s}$ = 13 TeV pp data-taking steadily increased from 88.8% to 97.5% between 2015 and 2018. This increase can be seen in the bottom panel of Figure 5.

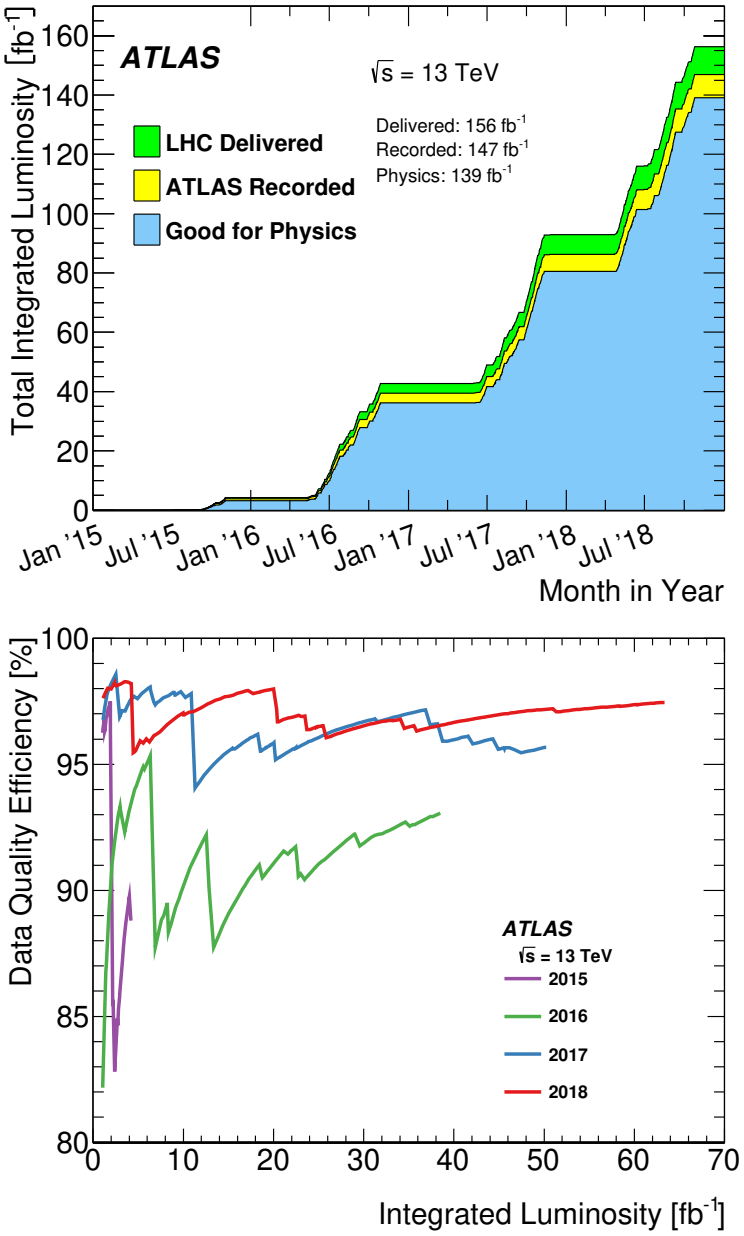


Figure 5: Top: Cumulative integrated luminosity delivered to and recorded by ATLAS between 2015 and 2018 during stable beam pp collision data-taking at $\sqrt{s}$ = 13 TeV. This includes machine commissioning periods, special runs for detector calibration, and LHC fills with a low number of circulating bunches or bunch spacing greater than 25 ns. Also shown is the cumulative integrated luminosity certified for physics analysis usage for the ATLAS experiment between 2015 and 2018 during standard pp collision data-taking at $\sqrt{s}$ = 13 TeV. The total integrated luminosity recorded for the standard $\sqrt{s}$ = 13 TeV pp collision dataset corresponds to 145 fb^{-1}. It is this number that is used in the denominator when calculating the data quality efficiency of the standard $\sqrt{s}$ = 13 TeV pp collision dataset. Bottom: Cumulative data quality efficiency versus total integrated luminosity delivered to the ATLAS experiment between 2015 and 2018.

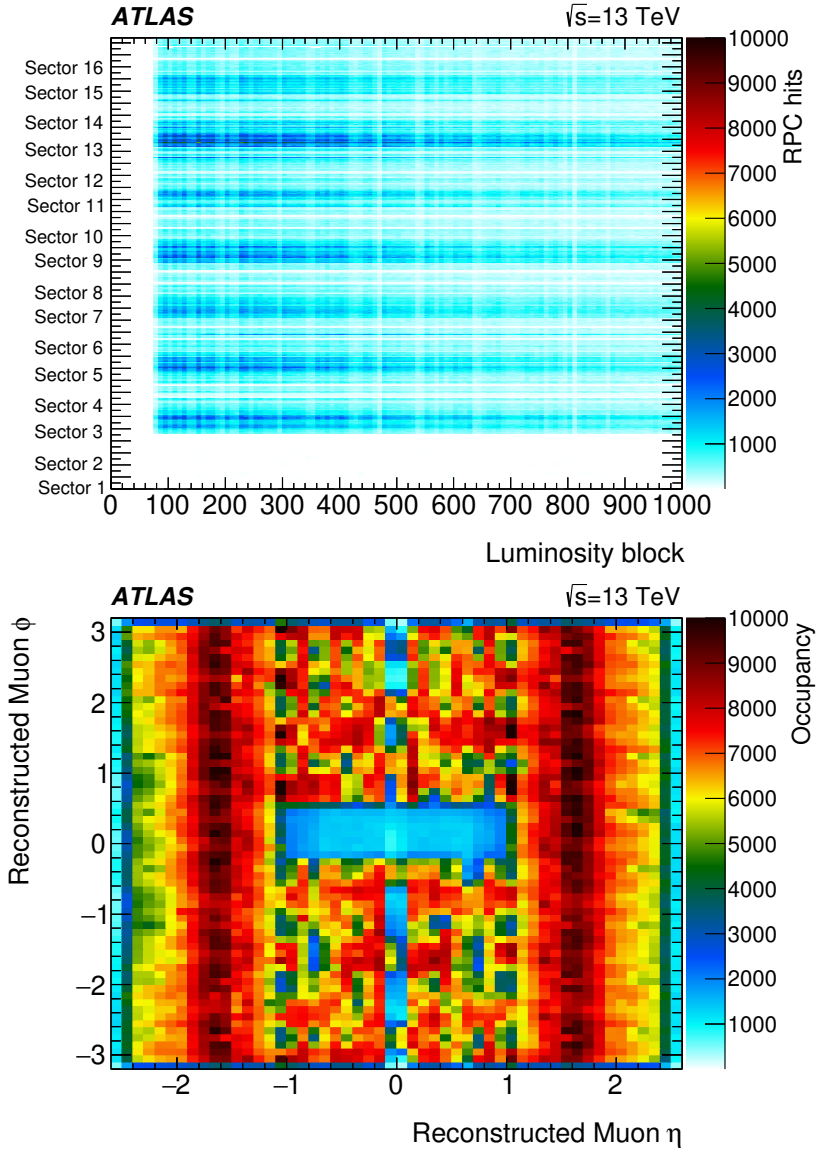


Figure 6: Illustration of an incident during 2017, which resulted in a significant loss of coverage for muons. Top: Number of hits in the various sectors of the RPC subsystem versus luminosity block, where the absence of entries for ϕ-sectors 1 and 2 indicates a hardware issue. Bottom: Occupancy of reconstructed muons in the η–ϕ plane, where the deficit in the range $-1 < \eta < 1$ at $\phi \sim 0$ illustrates the impact of this hardware problem on the reconstructed objects.

6 Summary

The ATLAS data quality operating scheme and assessment procedures as performed during LHC Run 2, and the data quality performance achieved as a result, are presented. The data quality performance for the standard pp collision dataset is presented, alongside the corresponding efficiency for special running periods, including heavy-ion data-taking and dedicated low-μ datasets. Data quality and ATLAS operating procedures have been subject to continuous review and development over the course of the Run 2 data-taking campaign, resulting in an increasing efficiency for good quality physics data. A data quality efficiency for the standard pp collision dataset collected at $\sqrt{s}$ = 13 TeV of 97.5% was achieved during 2018, completing a standard Run 2 dataset taken between 2015 and 2018 with a combined data quality efficiency of 95.6%.

Acknowledgements

We thank CERN for the very successful operation of the LHC, as well as the support staff from our institutions without whom ATLAS could not be operated efficiently.

We acknowledge the support of ANPCyT, Argentina; YerPhI, Armenia; ARC, Australia; BMWFW and FWF, Austria; ANAS, Azerbaijan; SSTC, Belarus; CNPq and FAPESP, Brazil; NSERC, NRC and CFI, Canada; CERN; CONICYT, Chile; CAS, MOST and NSFC, China; COLCIENCIAS, Colombia; MSMT CR, MPO CR and VSC CR, Czech Republic; DNRF and DNSRC, Denmark; IN2P3-CNRS and CEA-DRF/IRFU, France; SRNSFG, Georgia; BMBF, HGF and MPG, Germany; GSRT, Greece; RGC and Hong Kong SAR, China; ISF and Benoziyo Center, Israel; INFN, Italy; MEXT and JSPS, Japan; CNRST, Morocco; NWO, Netherlands; RCN, Norway; MNiSW and NCN, Poland; FCT, Portugal; MNE/IFA, Romania; MES of Russia and NRC KI, Russia Federation; JINR; MESTD, Serbia; MSSR, Slovakia; ARRS and MIZŠ, Slovenia; DST/NRF, South Africa; MINECO, Spain; SRC and Wallenberg Foundation, Sweden; SERI, SNSF and Cantons of Bern and Geneva, Switzerland; MOST, Taiwan; TAEK, Turkey; STFC, United Kingdom; DOE and NSF, United States of America. In addition, individual groups and members have received support from BCKDF, CANARIE, Compute Canada and CRC, Canada; ERC, ERDF, Horizon 2020, Marie Skłodowska-Curie Actions and COST, European Union; Investissements d'Avenir Labex, Investissements d'Avenir Idex and ANR, France; DFG and AvH Foundation, Germany; Herakleitos, Thales and Aristeia programmes co-financed by EU-ESF and the Greek NSRF, Greece; BSF-NSF and GIF, Israel; CERCA Programme Generalitat de Catalunya and PROMETEO Programme Generalitat Valenciana, Spain; Göran Gustafssons Stiftelse, Sweden; The Royal Society and Leverhulme Trust, United Kingdom.

The crucial computing support from all WLCG partners is acknowledged gratefully, in particular from CERN, the ATLAS Tier-1 facilities at TRIUMF (Canada), NDGF (Denmark, Norway, Sweden), CC-IN2P3 (France), KIT/GridKA (Germany), INFN-CNAF (Italy), NL-T1 (Netherlands), PIC (Spain), ASGC (Taiwan), RAL (UK) and BNL (USA), the Tier-2 facilities worldwide and large non-WLCG resource providers. Major contributors of computing resources are listed in Ref. [40].

References

[1] ATLAS Collaboration, *The ATLAS Experiment at the CERN Large Hadron Collider*, JINST **3** (2008) S08003.

[2] L. Evans and P. Bryant, *LHC Machine*, JINST **3** (2008) S08001.

[3] ATLAS Collaboration, *ATLAS Insertable B-Layer Technical Design Report*, ATLAS-TDR-19, 2010, URL: https://cds.cern.ch/record/1291633, Addendum: ATLAS-TDR-19-ADD-1, 2012, URL: https://cds.cern.ch/record/1451888.

[4] B. Abbott et al., *Production and integration of the ATLAS Insertable B-Layer*, JINST **13** (2018) T05008, arXiv: 1803.00844 [physics.ins-det].

[5] A. Collaboration, *Electron and photon performance measurements with the ATLAS detector using the 2015-2017 LHC proton-proton collision data*, 2019, arXiv: 1908.00005 [hep-ex].

[6] ATLAS Collaboration, *Muon reconstruction performance of the ATLAS detector in proton–proton collision data at* $\sqrt{s} = 13$ *TeV*, Eur. Phys. J. C **76** (2016) 292, arXiv: 1603.05598 [hep-ex].

[7] ATLAS Collaboration, *Measurement of the tau lepton reconstruction and identification performance in the ATLAS experiment using pp collisions at* $\sqrt{s} = 13$ *TeV*, ATLAS-CONF-2017-029, 2017, URL: https://cds.cern.ch/record/2261772.

[8] ATLAS Collaboration, *Properties of jets and inputs to jet reconstruction and calibration with the ATLAS detector using proton–proton collisions at* $\sqrt{s} = 13$ *TeV*, ATL-PHYS-PUB-2015-036, 2015, URL: https://cds.cern.ch/record/2044564.

[9] ATLAS Collaboration, *ATLAS b-jet identification performance and efficiency measurement with* $t\bar{t}$ *events in pp collisions at* $\sqrt{s} = 13$ *TeV*, (2019), arXiv: 1907.05120 [hep-ex].

[10] ATLAS Collaboration, E_T^{miss} *performance in the ATLAS detector using 2015–2016 LHC pp collisions*, ATLAS-CONF-2018-023, 2018, URL: https://cds.cern.ch/record/2625233.

[11] ATLAS Collaboration, *Performance of the ATLAS trigger system in 2015*, Eur. Phys. J. C **77** (2017) 317, arXiv: 1611.09661 [hep-ex].

[12] ATLAS Collaboration, *Luminosity determination in pp collisions at* $\sqrt{s} = 13$ *TeV using the ATLAS detector at the LHC*, ATLAS-CONF-2019-021, 2019, URL: https://cds.cern.ch/record/2677054.

[13] H. Wiedemann, *Particle Accelerator Physics*, Graduate Texts in Physics, Springer International Publishing, 2015, URL: https://www.springer.com/us/book/9783319183169?wt_mc=ThirdParty.SpringerLink.3.EPR653.About_eBook.

[14] G. Avoni et al., *The new LUCID-2 detector for luminosity measurement and monitoring in ATLAS*, JINST **13** (2018) P07017.

[15] H. Bertelsen et al., *Operation of the upgraded ATLAS Central Trigger Processor during the LHC Run 2*, JINST **11** (2016) C02020.

[16] M. Böhler, M. Borodin, A. Formica, E. Gallas and V. Radescu, *Evolution of ATLAS conditions data and its management for LHC Run-2*, J. Phys.: Conf. Ser. **664** (2015) 042005.

[17] M. Verducci, *ATLAS conditions database experience with the LCG COOL conditions database project*, J. Phys.: Conf. Ser. **119** (2008) 042031.

[18] R. Trentadue et al., *LCG Persistency Framework (CORAL, COOL, POOL): Status and Outlook in 2012*, J. Phys.: Conf. Ser. **396** (2012) 052067.

[19] I. Bird et al., *LHC computing Grid. Technical design report*, (2005), URL: http://cds.cern.ch/record/840543.

[20] A. Barriuso Poy et al., *The detector control system of the ATLAS experiment*, JINST **3** (2008) 05006.

[21] P. Adragna et al., *GNAM: a low-level monitoring program for the ATLAS experiment*, IEEE Trans. Nucl. Sci. **53** (2006) 1317.

[22] D. Salvatore et al., *The GNAM system in the ATLAS online monitoring framework*, Nucl. Phys. B Proc. Suppl. **172** (2007) 317.

[23] I. Scholtes, S. Kolos and P. F. Zema, *The ATLAS Event Monitoring Service - Peer-to-Peer Data Distribution in High-Energy Physics*, IEEE Trans. Nucl. Sci. **55** (3 2008) 1610.

[24] A. Corso-Radu et al., *Data Quality Monitoring Framework for the ATLAS experiment: Performance achieved with colliding beams at the LHC*, J. Phys.: Conf. Ser. **331** (2011) 022027.

[25] ATLAS TDAQ Collaboration, *The ATLAS Data Acquisition and High Level Trigger system*, JINST **11** (2016) 06008.

[26] A. Corso-Radu, *First-year experience with the ATLAS online monitoring framework*, J. Phys. Conf. Ser. **219** (2010) 022005.

[27] P. Renkel, H. Hadavand and R. Kehoe, *The Gatherer: a mechanism for integration of monitoring data in ATLAS*, J. Phys.: Conf. Ser. **219** (2010) 022043.

[28] Y. Ilchenko et al., *Data Quality Monitoring Display for ATLAS experiment at the LHC*, J. Phys.: Conf. Ser. **219** (2010) 022035.

[29] A. Dotti, P. Adragna and R. A. Vitillo, *The Online Histogram Presenter for the ATLAS experiment: A modular system for histogram visualization*, J. Phys.: Conf. Ser. **219** (2010) 032037.

[30] P. Zema, *The Monitoring Data Archiving Service for ATLAS*, IEEE Nucl. Scien. Symp. Conf. Rec. **6** (2007).

[31] ATLAS Collaboration, *Monitoring and data quality assessment of the ATLAS liquid argon calorimeter*, JINST **9** (2014) P07024, arXiv: 1405.3768 [hep-ex].

[32] ATLAS Collaboration, *Reconstruction of primary vertices at the ATLAS experiment in Run 1 proton–proton collisions at the LHC*, Eur. Phys. J. C **77** (2017) 332, arXiv: 1611.10235 [hep-ex].

[33] ATLAS Collaboration, *Alignment of the ATLAS Inner Detector with the initial LHC data at* $\sqrt{s} = 13$ *TeV*, ATL-PHYS-PUB-2015-031, 2015, URL: https://cds.cern.ch/record/2038139.

[34] T. Bray, J. Paoli, C. M. Sperberg-McQueen, E. Maler and F. Yergeau, *Extensible Markup Language (XML) 1.0 (Fifth Edition)*, W3C Recommendation, Available at http://www.w3.org/TR/REC-xml/, 2008.

[35] T. Golling, H. S. Hayward, P. U. E. Onyisi, H. J. Stelzer and P. Waller, *The ATLAS data quality defect database system*, Eur. Phys. J. C **72** (2012) 1960, arXiv: 1110.6119 [ins-det].

[36] R. Brun and F. Rademakers, *ROOT – An object oriented data analysis framework*, Nucl. Instrum. Meth. A **389** (1997) 81.

[37] ATLAS Collaboration, *Search for new phenomena in high-mass diphoton final states using* $37\,fb^{-1}$ *of proton–proton collisions collected at* $\sqrt{s} = 13$ *TeV with the ATLAS detector*, Phys. Lett. B **775** (2017) 105, arXiv: 1707.04147 [hep-ex].

[38] ATLAS Collaboration, *Search for diboson resonances with boson-tagged jets in pp collisions at $\sqrt{s} = 13$ TeV with the ATLAS detector*, Phys. Lett. B **777** (2018) 91, arXiv: 1708.04445 [hep-ex].

[39] ATLAS Collaboration, *A search for pair-produced resonances in four-jet final states at $\sqrt{s} = 13$ TeV with the ATLAS detector*, Eur. Phys. J. C **78** (2018) 250, arXiv: 1710.07171 [hep-ex].

[40] ATLAS Collaboration, *ATLAS Computing Acknowledgements*, ATL-GEN-PUB-2016-002, URL: https://cds.cern.ch/record/2202407.

The ATLAS Collaboration

G. Aad[102], B. Abbott[129], D.C. Abbott[103], A. Abed Abud[36], K. Abeling[53], D.K. Abhayasinghe[94], S.H. Abidi[167], O.S. AbouZeid[40], N.L. Abraham[156], H. Abramowicz[161], H. Abreu[160], Y. Abulaiti[6], B.S. Acharya[67a,67b,n], B. Achkar[53], S. Adachi[163], L. Adam[100], C. Adam Bourdarios[5], L. Adamczyk[84a], L. Adamek[167], J. Adelman[121], M. Adersberger[114], A. Adiguzel[12c], S. Adorni[54], T. Adye[144], A.A. Affolder[146], Y. Afik[160], C. Agapopoulou[65], M.N. Agaras[38], A. Aggarwal[119], C. Agheorghiesei[27c], J.A. Aguilar-Saavedra[140f,140a,ag], F. Ahmadov[80], W.S. Ahmed[104], X. Ai[18], G. Aielli[74a,74b], S. Akatsuka[86], T.P.A. Åkesson[97], E. Akilli[54], A.V. Akimov[111], K. Al Khoury[65], G.L. Alberghi[23b,23a], J. Albert[176], M.J. Alconada Verzini[161], S. Alderweireldt[36], M. Aleksa[36], I.N. Aleksandrov[80], C. Alexa[27b], T. Alexopoulos[10], A. Alfonsi[120], F. Alfonsi[23b,23a], M. Alhroob[129], B. Ali[142], M. Aliev[166], G. Alimonti[69a], S.P. Alkire[148], C. Allaire[65], B.M.M. Allbrooke[156], B.W. Allen[132], P.P. Allport[21], A. Aloisio[70a,70b], F. Alonso[89], C. Alpigiani[148], A.A. Alshehri[57], M. Alvarez Estevez[99], M.G. Alviggi[70a,70b], Y. Amaral Coutinho[81b], A. Ambler[104], L. Ambroz[135], C. Amelung[26], D. Amidei[106], S.P. Amor Dos Santos[140a], S. Amoroso[46], C.S. Amrouche[54], F. An[79], C. Anastopoulos[149], N. Andari[145], T. Andeen[11], C.F. Anders[61b], J.K. Anders[20], A. Andreazza[69a,69b], V. Andrei[61a], C.R. Anelli[176], S. Angelidakis[38], A. Angerami[39], A.V. Anisenkov[122b,122a], A. Annovi[72a], C. Antel[54], M.T. Anthony[149], E. Antipov[130], M. Antonelli[51], D.J.A. Antrim[171], F. Anulli[73a], M. Aoki[82], J.A. Aparisi Pozo[174], L. Aperio Bella[15a], J.P. Araque[140a], V. Araujo Ferraz[81b], R. Araujo Pereira[81b], C. Arcangeletti[51], A.T.H. Arce[49], F.A. Arduh[89], J-F. Arguin[110], S. Argyropoulos[78], J.-H. Arling[46], A.J. Armbruster[36], A. Armstrong[171], O. Arnaez[167], H. Arnold[120], Z.P. Arrubarrena Tame[114], G. Artoni[135], S. Artz[100], S. Asai[163], T. Asawatavonvanich[165], N. Asbah[59], E.M. Asimakopoulou[172], L. Asquith[156], J. Assahsah[35d], K. Assamagan[29], R. Astalos[28a], R.J. Atkin[33a], M. Atkinson[173], N.B. Atlay[19], H. Atmani[65], K. Augsten[142], G. Avolio[36], R. Avramidou[60a], M.K. Ayoub[15a], A.M. Azoulay[168b], G. Azuelos[110,ar], H. Bachacou[145], K. Bachas[68a,68b], M. Backes[135], F. Backman[45a,45b], P. Bagnaia[73a,73b], M. Bahmani[85], H. Bahrasemani[152], A.J. Bailey[174], V.R. Bailey[173], J.T. Baines[144], M. Bajic[40], C. Bakalis[10], O.K. Baker[183], P.J. Bakker[120], D. Bakshi Gupta[8], S. Balaji[157], E.M. Baldin[122b,122a], P. Balek[180], F. Balli[145], W.K. Balunas[135], J. Balz[100], E. Banas[85], A. Bandyopadhyay[24], Sw. Banerjee[181,i], A.A.E. Bannoura[182], L. Barak[161], W.M. Barbe[38], E.L. Barberio[105], D. Barberis[55b,55a], M. Barbero[102], G. Barbour[95], T. Barillari[115], M-S. Barisits[36], J. Barkeloo[132], T. Barklow[153], R. Barnea[160], S.L. Barnes[60c], B.M. Barnett[144], R.M. Barnett[18], Z. Barnovska-Blenessy[60a], A. Baroncelli[60a], G. Barone[29], A.J. Barr[135], L. Barranco Navarro[45a,45b], F. Barreiro[99], J. Barreiro Guimarães da Costa[15a], S. Barsov[138], R. Bartoldus[153], G. Bartolini[102], A.E. Barton[90], P. Bartos[28a], A. Basalaev[46], A. Basan[100], A. Bassalat[65,am], M.J. Basso[167], R.L. Bates[57], S. Batlamous[35e], J.R. Batley[32], B. Batool[151], M. Battaglia[146], M. Bauce[73a,73b], F. Bauer[145], K.T. Bauer[171], H.S. Bawa[31], J.B. Beacham[49], T. Beau[136], P.H. Beauchemin[170], F. Becherer[52], P. Bechtle[24], H.C. Beck[53], H.P. Beck[20,r], K. Becker[178], C. Becot[46], A. Beddall[12d], A.J. Beddall[12a], V.A. Bednyakov[80], M. Bedognetti[120], C.P. Bee[155], T.A. Beermann[182], M. Begalli[81b], M. Begel[29], A. Behera[155], J.K. Behr[46], F. Beisiegel[24], A.S. Bell[95], G. Bella[161], L. Bellagamba[23b], A. Bellerive[34], P. Bellos[9], K. Beloborodov[122b,122a], K. Belotskiy[112], N.L. Belyaev[112], D. Benchekroun[35a], N. Benekos[10], Y. Benhammou[161], D.P. Benjamin[6], M. Benoit[54], J.R. Bensinger[26], S. Bentvelsen[120], L. Beresford[135], M. Beretta[51], D. Berge[46], E. Bergeaas Kuutmann[172], N. Berger[5], B. Bergmann[142], L.J. Bergsten[26], J. Beringer[18], S. Berlendis[7], G. Bernardi[136], C. Bernius[153], F.U. Bernlochner[24], T. Berry[94], P. Berta[100], C. Bertella[15a], I.A. Bertram[90], O. Bessidskaia Bylund[182], N. Besson[145], A. Bethani[101], S. Bethke[115], A. Betti[42], A.J. Bevan[93], J. Beyer[115], D.S. Bhattacharya[177], P. Bhattarai[26], R. Bi[139], R.M. Bianchi[139], O. Biebel[114], D. Biedermann[19], R. Bielski[36], K. Bierwagen[100], N.V. Biesuz[72a,72b], M. Biglietti[75a], T.R.V. Billoud[110], M. Bindi[53], A. Bingul[12d], C. Bini[73a,73b], S. Biondi[23b,23a], M. Birman[180], T. Bisanz[53],

J.P. Biswal[161], D. Biswas[181,i], A. Bitadze[101], C. Bittrich[48], K. Bjørke[134], K.M. Black[25], T. Blazek[28a], I. Bloch[46], C. Blocker[26], A. Blue[57], U. Blumenschein[93], G.J. Bobbink[120], V.S. Bobrovnikov[122b,122a], S.S. Bocchetta[97], A. Bocci[49], D. Boerner[46], D. Bogavac[14], A.G. Bogdanchikov[122b,122a], C. Bohm[45a], V. Boisvert[94], P. Bokan[53,172], T. Bold[84a], A.S. Boldyrev[113], A.E. Bolz[61b], M. Bomben[136], M. Bona[93], J.S. Bonilla[132], M. Boonekamp[145], C.D. Booth[94], H.M. Borecka-Bielska[91], A. Borisov[123], G. Borissov[90], J. Bortfeldt[36], D. Bortoletto[135], D. Boscherini[23b], M. Bosman[14], J.D. Bossio Sola[104], K. Bouaouda[35a], J. Boudreau[139], E.V. Bouhova-Thacker[90], D. Boumediene[38], S.K. Boutle[57], A. Boveia[127], J. Boyd[36], D. Boye[33b,an], I.R. Boyko[80], A.J. Bozson[94], J. Bracinik[21], N. Brahimi[102], G. Brandt[182], O. Brandt[32], F. Braren[46], B. Brau[103], J.E. Brau[132], W.D. Breaden Madden[57], K. Brendlinger[46], L. Brenner[46], R. Brenner[172], S. Bressler[180], B. Brickwedde[100], D.L. Briglin[21], D. Britton[57], D. Britzger[115], I. Brock[24], R. Brock[107], G. Brooijmans[39], W.K. Brooks[147c], E. Brost[121], J.H Broughton[21], P.A. Bruckman de Renstrom[85], D. Bruncko[28b], A. Bruni[23b], G. Bruni[23b], L.S. Bruni[120], S. Bruno[74a,74b], M. Bruschi[23b], N. Bruscino[73a,73b], P. Bryant[37], L. Bryngemark[97], T. Buanes[17], Q. Buat[36], P. Buchholz[151], A.G. Buckley[57], I.A. Budagov[80], M.K. Bugge[134], F. Bührer[52], O. Bulekov[112], T.J. Burch[121], S. Burdin[91], C.D. Burgard[120], A.M. Burger[130], B. Burghgrave[8], J.T.P. Burr[46], C.D. Burton[11], J.C. Burzynski[103], V. Büscher[100], E. Buschmann[53], P.J. Bussey[57], J.M. Butler[25], C.M. Buttar[57], J.M. Butterworth[95], P. Butti[36], W. Buttinger[36], C.J. Buxo Vazquez[107], A. Buzatu[158], A.R. Buzykaev[122b,122a], G. Cabras[23b,23a], S. Cabrera Urbán[174], D. Caforio[56], H. Cai[173], V.M.M. Cairo[153], O. Cakir[4a], N. Calace[36], P. Calafiura[18], A. Calandri[102], G. Calderini[136], P. Calfayan[66], G. Callea[57], L.P. Caloba[81b], A. Caltabiano[74a,74b], S. Calvente Lopez[99], D. Calvet[38], S. Calvet[38], T.P. Calvet[155], M. Calvetti[72a,72b], R. Camacho Toro[136], S. Camarda[36], D. Camarero Munoz[99], P. Camarri[74a,74b], D. Cameron[134], R. Caminal Armadans[103], C. Camincher[36], S. Campana[36], M. Campanelli[95], A. Camplani[40], A. Campoverde[151], V. Canale[70a,70b], A. Canesse[104], M. Cano Bret[60c], J. Cantero[130], T. Cao[161], Y. Cao[173], M.D.M. Capeans Garrido[36], M. Capua[41b,41a], R. Cardarelli[74a], F. Cardillo[149], G. Carducci[41b,41a], I. Carli[143], T. Carli[36], G. Carlino[70a], B.T. Carlson[139], L. Carminati[69a,69b], R.M.D. Carney[45a,45b], S. Caron[119], E. Carquin[147c], S. Carrá[46], J.W.S. Carter[167], M.P. Casado[14,e], A.F. Casha[167], D.W. Casper[171], R. Castelijn[120], F.L. Castillo[174], L. Castillo Garcia[14], V. Castillo Gimenez[174], N.F. Castro[140a,140e], A. Catinaccio[36], J.R. Catmore[134], A. Cattai[36], V. Cavaliere[29], E. Cavallaro[14], M. Cavalli-Sforza[14], V. Cavasinni[72a,72b], E. Celebi[12b], L. Cerda Alberich[174], K. Cerny[131], A.S. Cerqueira[81a], A. Cerri[156], L. Cerrito[74a,74b], F. Cerutti[18], A. Cervelli[23b,23a], S.A. Cetin[12b], Z. Chadi[35a], D. Chakraborty[121], W.S. Chan[120], W.Y. Chan[91], J.D. Chapman[32], B. Chargeishvili[159b], D.G. Charlton[21], T.P. Charman[93], C.C. Chau[34], S. Che[127], S. Chekanov[6], S.V. Chekulaev[168a], G.A. Chelkov[80,aq], M.A. Chelstowska[36], B. Chen[79], C. Chen[60a], C.H. Chen[79], H. Chen[29], J. Chen[60a], J. Chen[39], J. Chen[26], S. Chen[137], S.J. Chen[15c], X. Chen[15b], Y-H. Chen[46], H.C. Cheng[63a], H.J. Cheng[15a], A. Cheplakov[80], E. Cheremushkina[123], R. Cherkaoui El Moursli[35e], E. Cheu[7], K. Cheung[64], T.J.A. Chevalérias[145], L. Chevalier[145], V. Chiarella[51], G. Chiarelli[72a], G. Chiodini[68a], A.S. Chisholm[21], A. Chitan[27b], I. Chiu[163], Y.H. Chiu[176], M.V. Chizhov[80], K. Choi[11], A.R. Chomont[73a,73b], S. Chouridou[162], Y.S. Chow[120], M.C. Chu[63a], X. Chu[15a,15d], J. Chudoba[141], A.J. Chuinard[104], J.J. Chwastowski[85], L. Chytka[131], D. Cieri[115], K.M. Ciesla[85], D. Cinca[47], V. Cindro[92], I.A. Cioară[27b], A. Ciocio[18], F. Cirotto[70a,70b], Z.H. Citron[180,j], M. Citterio[69a], D.A. Ciubotaru[27b], B.M. Ciungu[167], A. Clark[54], M.R. Clark[39], P.J. Clark[50], C. Clement[45a,45b], Y. Coadou[102], M. Cobal[67a,67c], A. Coccaro[55b], J. Cochran[79], H. Cohen[161], A.E.C. Coimbra[36], L. Colasurdo[119], B. Cole[39], A.P. Colijn[120], J. Collot[58], P. Conde Muiño[140a,140h], S.H. Connell[33b], I.A. Connelly[57], S. Constantinescu[27b], F. Conventi[70a,as], A.M. Cooper-Sarkar[135], F. Cormier[175], K.J.R. Cormier[167], L.D. Corpe[95], M. Corradi[73a,73b], E.E. Corrigan[97], F. Corriveau[104,ae], A. Cortes-Gonzalez[36], M.J. Costa[174], F. Costanza[5], D. Costanzo[149], G. Cowan[94], J.W. Cowley[32], J. Crane[101], K. Cranmer[125], S.J. Crawley[57], R.A. Creager[137], S. Crépé-Renaudin[58], F. Crescioli[136], M. Cristinziani[24], V. Croft[170], G. Crosetti[41b,41a], A. Cueto[5], T. Cuhadar Donszelmann[149],

A.R. Cukierman[153], W.R. Cunningham[57], S. Czekierda[85], P. Czodrowski[36], M.J. Da Cunha Sargedas De Sousa[60b], J.V. Da Fonseca Pinto[81b], C. Da Via[101], W. Dabrowski[84a], F. Dachs[36], T. Dado[28a], S. Dahbi[35e], T. Dai[106], C. Dallapiccola[103], M. Dam[40], G. D'amen[29], V. D'Amico[75a,75b], J. Damp[100], J.R. Dandoy[137], M.F. Daneri[30], N.P. Dang[181,i], N.S. Dann[101], M. Danninger[175], V. Dao[36], G. Darbo[55b], O. Dartsi[5], A. Dattagupta[132], T. Daubney[46], S. D'Auria[69a,69b], C. David[168b], T. Davidek[143], D.R. Davis[49], I. Dawson[149], K. De[8], R. De Asmundis[70a], M. De Beurs[120], S. De Castro[23b,23a], S. De Cecco[73a,73b], N. De Groot[119], P. de Jong[120], H. De la Torre[107], A. De Maria[15c], D. De Pedis[73a], A. De Salvo[73a], U. De Sanctis[74a,74b], M. De Santis[74a,74b], A. De Santo[156], K. De Vasconcelos Corga[102], J.B. De Vivie De Regie[65], C. Debenedetti[146], D.V. Dedovich[80], A.M. Deiana[42], J. Del Peso[99], Y. Delabat Diaz[46], D. Delgove[65], F. Deliot[145,q], C.M. Delitzsch[7], M. Della Pietra[70a,70b], D. Della Volpe[54], A. Dell'Acqua[36], L. Dell'Asta[74a,74b], M. Delmastro[5], C. Delporte[65], P.A. Delsart[58], D.A. DeMarco[167], S. Demers[183], M. Demichev[80], G. Demontigny[110], S.P. Denisov[123], L. D'Eramo[136], D. Derendarz[85], J.E. Derkaoui[35d], F. Derue[136], P. Dervan[91], K. Desch[24], C. Deterre[46], K. Dette[167], C. Deutsch[24], M.R. Devesa[30], P.O. Deviveiros[36], A. Dewhurst[144], F.A. Di Bello[54], A. Di Ciaccio[74a,74b], L. Di Ciaccio[5], W.K. Di Clemente[137], C. Di Donato[70a,70b], A. Di Girolamo[36], G. Di Gregorio[72a,72b], B. Di Micco[75a,75b], R. Di Nardo[75a,75b], K.F. Di Petrillo[59], R. Di Sipio[167], D. Di Valentino[34], C. Diaconu[102], F.A. Dias[40], T. Dias Do Vale[140a], M.A. Diaz[147a], J. Dickinson[18], E.B. Diehl[106], J. Dietrich[19], S. Díez Cornell[46], A. Dimitrievska[18], W. Ding[15b], J. Dingfelder[24], F. Dittus[36], F. Djama[102], T. Djobava[159b], J.I. Djuvsland[17], M.A.B. Do Vale[81c], M. Dobre[27b], D. Dodsworth[26], C. Doglioni[97], J. Dolejsi[143], Z. Dolezal[143], M. Donadelli[81d], B. Dong[60c], J. Donini[38], A. D'onofrio[15c], M. D'Onofrio[91], J. Dopke[144], A. Doria[70a], M.T. Dova[89], A.T. Doyle[57], E. Drechsler[152], E. Dreyer[152], T. Dreyer[53], A.S. Drobac[170], D. Du[60b], Y. Duan[60b], F. Dubinin[111], M. Dubovsky[28a], A. Dubreuil[54], E. Duchovni[180], G. Duckeck[114], A. Ducourthial[136], O.A. Ducu[110], D. Duda[115], A. Dudarev[36], A.C. Dudder[100], E.M. Duffield[18], L. Duflot[65], M. Dührssen[36], C. Dülsen[182], M. Dumancic[180], A.E. Dumitriu[27b], A.K. Duncan[57], M. Dunford[61a], A. Duperrin[102], H. Duran Yildiz[4a], M. Düren[56], A. Durglishvili[159b], D. Duschinger[48], B. Dutta[46], D. Duvnjak[1], G.I. Dyckes[137], M. Dyndal[36], S. Dysch[101], B.S. Dziedzic[85], K.M. Ecker[115], R.C. Edgar[106], M.G. Eggleston[49], T. Eifert[8], G. Eigen[17], K. Einsweiler[18], T. Ekelof[172], H. El Jarrari[35e], R. El Kosseifi[102], V. Ellajosyula[172], M. Ellert[172], F. Ellinghaus[182], A.A. Elliot[93], N. Ellis[36], J. Elmsheuser[29], M. Elsing[36], D. Emeliyanov[144], A. Emerman[39], Y. Enari[163], M.B. Epland[49], J. Erdmann[47], A. Ereditato[20], M. Errenst[36], M. Escalier[65], C. Escobar[174], O. Estrada Pastor[174], E. Etzion[161], H. Evans[66], A. Ezhilov[138], F. Fabbri[57], L. Fabbri[23b,23a], V. Fabiani[119], G. Facini[95], R.M. Faisca Rodrigues Pereira[140a], R.M. Fakhrutdinov[123], S. Falciano[73a], P.J. Falke[5], S. Falke[5], J. Faltova[143], Y. Fang[15a], Y. Fang[15a], G. Fanourakis[44], M. Fanti[69a,69b], M. Faraj[67a,67c,t], A. Farbin[8], A. Farilla[75a], E.M. Farina[71a,71b], T. Farooque[107], S. Farrell[18], S.M. Farrington[50], P. Farthouat[36], F. Fassi[35e], P. Fassnacht[36], D. Fassouliotis[9], M. Faucci Giannelli[50], W.J. Fawcett[32], L. Fayard[65], O.L. Fedin[138,o], W. Fedorko[175], A. Fehr[20], M. Feickert[173], L. Feligioni[102], A. Fell[149], C. Feng[60b], M. Feng[49], M.J. Fenton[57], A.B. Fenyuk[123], S.W. Ferguson[43], J. Ferrando[46], A. Ferrante[173], A. Ferrari[172], P. Ferrari[120], R. Ferrari[71a], D.E. Ferreira de Lima[61b], A. Ferrer[174], D. Ferrere[54], C. Ferretti[106], F. Fiedler[100], A. Filipčič[92], F. Filthaut[119], K.D. Finelli[25], M.C.N. Fiolhais[140a,140c,a], L. Fiorini[174], F. Fischer[114], W.C. Fisher[107], I. Fleck[151], P. Fleischmann[106], R.R.M. Fletcher[137], T. Flick[182], B.M. Flierl[114], L. Flores[137], L.R. Flores Castillo[63a], F.M. Follega[76a,76b], N. Fomin[17], J.H. Foo[167], G.T. Forcolin[76a,76b], A. Formica[145], F.A. Förster[14], A.C. Forti[101], A.G. Foster[21], M.G. Foti[135], D. Fournier[65], H. Fox[90], P. Francavilla[72a,72b], S. Francescato[73a,73b], M. Franchini[23b,23a], S. Franchino[61a], D. Francis[36], L. Franconi[20], M. Franklin[59], A.N. Fray[93], P.M. Freeman[21], B. Freund[110], W.S. Freund[81b], E.M. Freundlich[47], D.C. Frizzell[129], D. Froidevaux[36], J.A. Frost[135], C. Fukunaga[164], E. Fullana Torregrosa[174], E. Fumagalli[55b,55a], T. Fusayasu[116], J. Fuster[174], A. Gabrielli[23b,23a], A. Gabrielli[18], S. Gadatsch[54], P. Gadow[115], G. Gagliardi[55b,55a], L.G. Gagnon[110], C. Galea[27b], B. Galhardo[140a], G.E. Gallardo[135], E.J. Gallas[135],

B.J. Gallop[144], G. Galster[40], R. Gamboa Goni[93], K.K. Gan[127], S. Ganguly[180], J. Gao[60a], Y. Gao[50], Y.S. Gao[31,l], C. García[174], J.E. García Navarro[174], J.A. García Pascual[15a], C. Garcia-Argos[52], M. Garcia-Sciveres[18], R.W. Gardner[37], N. Garelli[153], S. Gargiulo[52], C.A. Garner[167], V. Garonne[134], S.J. Gasiorowski[148], P. Gaspar[81b], A. Gaudiello[55b,55a], G. Gaudio[71a], I.L. Gavrilenko[111], A. Gavrilyuk[124], C. Gay[175], G. Gaycken[46], E.N. Gazis[10], A.A. Geanta[27b], C.M. Gee[146], C.N.P. Gee[144], J. Geisen[53], M. Geisen[100], C. Gemme[55b], M.H. Genest[58], C. Geng[106], S. Gentile[73a,73b], S. George[94], T. Geralis[44], L.O. Gerlach[53], P. Gessinger-Befurt[100], G. Gessner[47], S. Ghasemi[151], M. Ghasemi Bostanabad[176], M. Ghneimat[151], A. Ghosh[65], A. Ghosh[78], B. Giacobbe[23b], S. Giagu[73a,73b], N. Giangiacomi[23b,23a], P. Giannetti[72a], A. Giannini[70a,70b], G. Giannini[14], S.M. Gibson[94], M. Gignac[146], D. Gillberg[34], G. Gilles[182], D.M. Gingrich[3,ar], M.P. Giordani[67a,67c], P.F. Giraud[145], G. Giugliarelli[67a,67c], D. Giugni[69a], F. Giuli[74a,74b], S. Gkaitatzis[162], I. Gkialas[9,g], E.L. Gkougkousis[14], P. Gkountoumis[10], L.K. Gladilin[113], C. Glasman[99], J. Glatzer[14], P.C.F. Glaysher[46], A. Glazov[46], G.R. Gledhill[132], M. Goblirsch-Kolb[26], D. Godin[110], S. Goldfarb[105], T. Golling[54], D. Golubkov[123], A. Gomes[140a,140b], R. Goncalves Gama[53], R. Gonçalo[140a], G. Gonella[52], L. Gonella[21], A. Gongadze[80], F. Gonnella[21], J.L. Gonski[39], S. González de la Hoz[174], S. Gonzalez-Sevilla[54], G.R. Gonzalvo Rodriguez[174], L. Goossens[36], N.A. Gorasia[21], P.A. Gorbounov[124], H.A. Gordon[29], B. Gorini[36], E. Gorini[68a,68b], A. Gorišek[92], A.T. Goshaw[49], M.I. Gostkin[80], C.A. Gottardo[119], M. Gouighri[35b], A.G. Goussiou[148], N. Govender[33b], C. Goy[5], E. Gozani[160], I. Grabowska-Bold[84a], E.C. Graham[91], J. Gramling[171], E. Gramstad[134], S. Grancagnolo[19], M. Grandi[156], V. Gratchev[138], P.M. Gravila[27f], F.G. Gravili[68a,68b], C. Gray[57], H.M. Gray[18], C. Grefe[24], K. Gregersen[97], I.M. Gregor[46], P. Grenier[153], K. Grevtsov[46], C. Grieco[14], N.A. Grieser[129], A.A. Grillo[146], K. Grimm[31,k], S. Grinstein[14,z], J.-F. Grivaz[65], S. Groh[100], E. Gross[180], J. Grosse-Knetter[53], Z.J. Grout[95], C. Grud[106], A. Grummer[118], L. Guan[106], W. Guan[181], C. Gubbels[175], J. Guenther[36], A. Guerguichon[65], J.G.R. Guerrero Rojas[174], F. Guescini[115], D. Guest[171], R. Gugel[52], T. Guillemin[5], S. Guindon[36], U. Gul[57], J. Guo[60c], W. Guo[106], Y. Guo[60a,s], Z. Guo[102], R. Gupta[46], S. Gurbuz[12c], G. Gustavino[129], M. Guth[52], P. Gutierrez[129], C. Gutschow[95], C. Guyot[145], C. Gwenlan[135], C.B. Gwilliam[91], A. Haas[125], C. Haber[18], H.K. Hadavand[8], A. Hadef[60a], S. Hageböck[36], M. Haleem[177], J. Haley[130], G. Halladjian[107], G.D. Hallewell[102], K. Hamacher[182], P. Hamal[131], K. Hamano[176], H. Hamdaoui[35e], M. Hamer[24], G.N. Hamity[50], K. Han[60a,y], L. Han[60a], S. Han[15a], Y.F. Han[167], K. Hanagaki[82,w], M. Hance[146], D.M. Handl[114], B. Haney[137], R. Hankache[136], E. Hansen[97], J.B. Hansen[40], J.D. Hansen[40], M.C. Hansen[24], P.H. Hansen[40], E.C. Hanson[101], K. Hara[169], T. Harenberg[182], S. Harkusha[108], P.F. Harrison[178], N.M. Hartmann[114], Y. Hasegawa[150], A. Hasib[50], S. Hassani[145], S. Haug[20], R. Hauser[107], L.B. Havener[39], M. Havranek[142], C.M. Hawkes[21], R.J. Hawkings[36], D. Hayden[107], C. Hayes[106], R.L. Hayes[175], C.P. Hays[135], J.M. Hays[93], H.S. Hayward[91], S.J. Haywood[144], F. He[60a], M.P. Heath[50], V. Hedberg[97], L. Heelan[8], S. Heer[24], K.K. Heidegger[52], W.D. Heidorn[79], J. Heilman[34], S. Heim[46], T. Heim[18], B. Heinemann[46,ao], J.J. Heinrich[132], L. Heinrich[36], J. Hejbal[141], L. Helary[61b], A. Held[175], S. Hellesund[134], C.M. Helling[146], S. Hellman[45a,45b], C. Helsens[36], R.C.W. Henderson[90], Y. Heng[181], L. Henkelmann[61a], S. Henkelmann[175], A.M. Henriques Correia[36], H. Herde[26], V. Herget[177], Y. Hernández Jiménez[33d], H. Herr[100], M.G. Herrmann[114], T. Herrmann[48], G. Herten[52], R. Hertenberger[114], L. Hervas[36], T.C. Herwig[137], G.G. Hesketh[95], N.P. Hessey[168a], A. Higashida[163], S. Higashino[82], E. Higón-Rodriguez[174], K. Hildebrand[37], J.C. Hill[32], K.K. Hill[29], K.H. Hiller[46], S.J. Hillier[21], M. Hils[48], I. Hinchliffe[18], F. Hinterkeuser[24], M. Hirose[133], S. Hirose[52], D. Hirschbuehl[182], B. Hiti[92], O. Hladik[141], D.R. Hlaluku[33d], X. Hoad[50], J. Hobbs[155], N. Hod[180], M.C. Hodgkinson[149], A. Hoecker[36], D. Hohn[52], D. Hohov[65], T. Holm[24], T.R. Holmes[37], M. Holzbock[114], L.B.A.H. Hommels[32], S. Honda[169], T.M. Hong[139], J.C. Honig[52], A. Hönle[115], B.H. Hooberman[173], W.H. Hopkins[6], Y. Horii[117], P. Horn[48], L.A. Horyn[37], S. Hou[158], A. Hoummada[35a], J. Howarth[101], J. Hoya[89], M. Hrabovsky[131], J. Hrdinka[77], I. Hristova[19], J. Hrivnac[65], A. Hrynevich[109], T. Hryn'ova[5], P.J. Hsu[64], S.-C. Hsu[148], Q. Hu[29], S. Hu[60c], Y.F. Hu[15a,15d], D.P. Huang[95], Y. Huang[60a], Y. Huang[15a],

Z. Hubacek[142], F. Hubaut[102], M. Huebner[24], F. Huegging[24], T.B. Huffman[135], M. Huhtinen[36], R.F.H. Hunter[34], P. Huo[155], N. Huseynov[80,af], J. Huston[107], J. Huth[59], R. Hyneman[106], S. Hyrych[28a], G. Iacobucci[54], G. Iakovidis[29], I. Ibragimov[151], L. Iconomidou-Fayard[65], P. Iengo[36], R. Ignazzi[40], O. Igonkina[120,ab,*], R. Iguchi[163], T. Iizawa[54], Y. Ikegami[82], M. Ikeno[82], D. Iliadis[162], N. Ilic[119,167,ae], F. Iltzsche[48], G. Introzzi[71a,71b], M. Iodice[75a], K. Iordanidou[168a], V. Ippolito[73a,73b], M.F. Isacson[172], M. Ishino[163], W. Islam[130], C. Issever[19,46], S. Istin[160], F. Ito[169], J.M. Iturbe Ponce[63a], R. Iuppa[76a,76b], A. Ivina[180], H. Iwasaki[82], J.M. Izen[43], V. Izzo[70a], P. Jacka[141], P. Jackson[1], R.M. Jacobs[24], B.P. Jaeger[152], V. Jain[2], G. Jäkel[182], K.B. Jakobi[100], K. Jakobs[52], T. Jakoubek[141], J. Jamieson[57], K.W. Janas[84a], R. Jansky[54], J. Janssen[24], M. Janus[53], P.A. Janus[84a], G. Jarlskog[97], N. Javadov[80,af], T. Javůrek[36], M. Javurkova[103], F. Jeanneau[145], L. Jeanty[132], J. Jejelava[159a], A. Jelinskas[178], P. Jenni[52,b], J. Jeong[46], N. Jeong[46], S. Jézéquel[5], H. Ji[181], J. Jia[155], H. Jiang[79], Y. Jiang[60a], Z. Jiang[153,p], S. Jiggins[52], F.A. Jimenez Morales[38], J. Jimenez Pena[115], S. Jin[15c], A. Jinaru[27b], O. Jinnouchi[165], H. Jivan[33d], P. Johansson[149], K.A. Johns[7], C.A. Johnson[66], R.W.L. Jones[90], S.D. Jones[156], S. Jones[7], T.J. Jones[91], J. Jongmanns[61a], P.M. Jorge[140a], J. Jovicevic[36], X. Ju[18], J.J. Junggeburth[115], A. Juste Rozas[14,z], A. Kaczmarska[85], M. Kado[73a,73b], H. Kagan[127], M. Kagan[153], A. Kahn[39], C. Kahra[100], T. Kaji[179], E. Kajomovitz[160], C.W. Kalderon[97], A. Kaluza[100], A. Kamenshchikov[123], M. Kaneda[163], N.J. Kang[146], S. Kang[79], L. Kanjir[92], Y. Kano[117], V.A. Kantserov[112], J. Kanzaki[82], L.S. Kaplan[181], D. Kar[33d], K. Karava[135], M.J. Kareem[168b], S.N. Karpov[80], Z.M. Karpova[80], V. Kartvelishvili[90], A.N. Karyukhin[123], L. Kashif[181], R.D. Kass[127], A. Kastanas[45a,45b], C. Kato[60d,60c], J. Katzy[46], K. Kawade[150], K. Kawagoe[88], T. Kawaguchi[117], T. Kawamoto[145], G. Kawamura[53], E.F. Kay[176], V.F. Kazanin[122b,122a], R. Keeler[176], R. Kehoe[42], J.S. Keller[34], E. Kellermann[97], D. Kelsey[156], J.J. Kempster[21], J. Kendrick[21], K.E. Kennedy[39], O. Kepka[141], S. Kersten[182], B.P. Kerševan[92], S. Ketabchi Haghighat[167], M. Khader[173], F. Khalil-Zada[13], M. Khandoga[145], A. Khanov[130], A.G. Kharlamov[122b,122a], T. Kharlamova[122b,122a], E.E. Khoda[175], A. Khodinov[166], T.J. Khoo[54], E. Khramov[80], J. Khubua[159b], S. Kido[83], M. Kiehn[54], C.R. Kilby[94], Y.K. Kim[37], N. Kimura[95], O.M. Kind[19], B.T. King[91,*], D. Kirchmeier[48], J. Kirk[144], A.E. Kiryunin[115], T. Kishimoto[163], D.P. Kisliuk[167], V. Kitali[46], O. Kivernyk[5], T. Klapdor-Kleingrothaus[52], M. Klassen[61a], M.H. Klein[106], M. Klein[91], U. Klein[91], K. Kleinknecht[100], P. Klimek[121], A. Klimentov[29], T. Klingl[24], T. Klioutchnikova[36], F.F. Klitzner[114], P. Kluit[120], S. Kluth[115], E. Kneringer[77], E.B.F.G. Knoops[102], A. Knue[52], D. Kobayashi[88], T. Kobayashi[163], M. Kobel[48], M. Kocian[153], T. Kodama[163], P. Kodys[143], P.T. Koenig[24], T. Koffas[34], N.M. Köhler[36], T. Koi[153], M. Kolb[145], I. Koletsou[5], T. Komarek[131], T. Kondo[82], K. Köneke[52], A.X.Y. Kong[1], A.C. König[119], T. Kono[126], R. Konoplich[125,aj], V. Konstantinides[95], N. Konstantinidis[95], B. Konya[97], R. Kopeliansky[66], S. Koperny[84a], K. Korcyl[85], K. Kordas[162], G. Koren[161], A. Korn[95], I. Korolkov[14], E.V. Korolkova[149], N. Korotkova[113], O. Kortner[115], S. Kortner[115], T. Kosek[143], V.V. Kostyukhin[149,166], A. Kotsokechagia[65], A. Kotwal[49], A. Koulouris[10], A. Kourkoumeli-Charalampidi[71a,71b], C. Kourkoumelis[9], E. Kourlitis[149], V. Kouskoura[29], A.B. Kowalewska[85], R. Kowalewski[176], C. Kozakai[163], W. Kozanecki[145], A.S. Kozhin[123], V.A. Kramarenko[113], G. Kramberger[92], D. Krasnopevtsev[60a], M.W. Krasny[136], A. Krasznahorkay[36], D. Krauss[115], J.A. Kremer[84a], J. Kretzschmar[91], P. Krieger[167], F. Krieter[114], A. Krishnan[61b], K. Krizka[18], K. Kroeninger[47], H. Kroha[115], J. Kroll[141], J. Kroll[137], K.S. Krowpman[107], J. Krstic[16], U. Kruchonak[80], H. Krüger[24], N. Krumnack[79], M.C. Kruse[49], J.A. Krzysiak[85], T. Kubota[105], O. Kuchinskaia[166], S. Kuday[4b], J.T. Kuechler[46], S. Kuehn[36], A. Kugel[61a], T. Kuhl[46], V. Kukhtin[80], R. Kukla[102], Y. Kulchitsky[108,ah], S. Kuleshov[147c], Y.P. Kulinich[173], M. Kuna[58], T. Kunigo[86], A. Kupco[141], T. Kupfer[47], O. Kuprash[52], H. Kurashige[83], L.L. Kurchaninov[168a], Y.A. Kurochkin[108], A. Kurova[112], M.G. Kurth[15a,15d], E.S. Kuwertz[36], M. Kuze[165], A.K. Kvam[148], J. Kvita[131], T. Kwan[104], A. La Rosa[115], L. La Rotonda[41b,41a], F. La Ruffa[41b,41a], C. Lacasta[174], F. Lacava[73a,73b], D.P.J. Lack[101], H. Lacker[19], D. Lacour[136], E. Ladygin[80], R. Lafaye[5], B. Laforge[136], T. Lagouri[33d], S. Lai[53], I.K. Lakomiec[84a], S. Lammers[66], W. Lampl[7], C. Lampoudis[162], E. Lançon[29], U. Landgraf[52], M.P.J. Landon[93], M.C. Lanfermann[54], V.S. Lang[46],

J.C. Lange[53], R.J. Langenberg[103], A.J. Lankford[171], F. Lanni[29], K. Lantzsch[24], A. Lanza[71a], A. Lapertosa[55b,55a], S. Laplace[136], J.F. Laporte[145], T. Lari[69a], F. Lasagni Manghi[23b,23a], M. Lassnig[36], T.S. Lau[63a], A. Laudrain[65], A. Laurier[34], M. Lavorgna[70a,70b], S.D. Lawlor[94], M. Lazzaroni[69a,69b], B. Le[105], E. Le Guirriec[102], M. LeBlanc[7], T. LeCompte[6], F. Ledroit-Guillon[58], A.C.A. Lee[95], C.A. Lee[29], G.R. Lee[17], L. Lee[59], S.C. Lee[158], S.J. Lee[34], S. Lee[79], B. Lefebvre[168a], H.P. Lefebvre[94], M. Lefebvre[176], C. Leggett[18], K. Lehmann[152], N. Lehmann[182], G. Lehmann Miotto[36], W.A. Leight[46], A. Leisos[162,x], M.A.L. Leite[81d], C.E. Leitgeb[114], R. Leitner[143], D. Lellouch[180,*], K.J.C. Leney[42], T. Lenz[24], R. Leone[7], S. Leone[72a], C. Leonidopoulos[50], A. Leopold[136], C. Leroy[110], R. Les[167], C.G. Lester[32], M. Levchenko[138], J. Levêque[5], D. Levin[106], L.J. Levinson[180], D.J. Lewis[21], B. Li[15b], B. Li[106], C-Q. Li[60a], F. Li[60c], H. Li[60a], H. Li[60b], J. Li[60c], K. Li[153], L. Li[60c], M. Li[15a,15d], Q. Li[15a,15d], Q.Y. Li[60a], S. Li[60d,60c], X. Li[46], Y. Li[46], Z. Li[60b], Z. Liang[15a], B. Liberti[74a], A. Liblong[167], K. Lie[63c], S. Lim[29], C.Y. Lin[32], K. Lin[107], T.H. Lin[100], R.A. Linck[66], J.H. Lindon[21], A.L. Lionti[54], E. Lipeles[137], A. Lipniacka[17], T.M. Liss[173,ap], A. Lister[175], J.D. Little[8], B. Liu[79], B.L. Liu[6], H.B. Liu[29], H. Liu[106], J.B. Liu[60a], J.K.K. Liu[37], K. Liu[136], M. Liu[60a], P. Liu[18], Y. Liu[15a,15d], Y.L. Liu[106], Y.W. Liu[60a], M. Livan[71a,71b], A. Lleres[58], J. Llorente Merino[152], S.L. Lloyd[93], C.Y. Lo[63b], F. Lo Sterzo[42], E.M. Lobodzinska[46], P. Loch[7], S. Loffredo[74a,74b], T. Lohse[19], K. Lohwasser[149], M. Lokajicek[141], J.D. Long[173], R.E. Long[90], L. Longo[36], K.A. Looper[127], J.A. Lopez[147c], I. Lopez Paz[101], A. Lopez Solis[149], J. Lorenz[114], N. Lorenzo Martinez[5], A.M. Lory[114], M. Losada[22], P.J. Lösel[114], A. Lösle[52], X. Lou[46], X. Lou[15a], A. Lounis[65], J. Love[6], P.A. Love[90], J.J. Lozano Bahilo[174], M. Lu[60a], Y.J. Lu[64], H.J. Lubatti[148], C. Luci[73a,73b], A. Lucotte[58], C. Luedtke[52], F. Luehring[66], I. Luise[136], L. Luminari[73a], B. Lund-Jensen[154], M.S. Lutz[103], D. Lynn[29], H. Lyons[91], R. Lysak[141], E. Lytken[97], F. Lyu[15a], V. Lyubushkin[80], T. Lyubushkina[80], H. Ma[29], L.L. Ma[60b], Y. Ma[60b], G. Maccarrone[51], A. Macchiolo[115], C.M. Macdonald[149], J. Machado Miguens[137], D. Madaffari[174], R. Madar[38], W.F. Mader[48], M. Madugoda Ralalage Don[130], N. Madysa[48], J. Maeda[83], T. Maeno[29], M. Maerker[48], A.S. Maevskiy[113], V. Magerl[52], N. Magini[79], D.J. Mahon[39], C. Maidantchik[81b], T. Maier[114], A. Maio[140a,140b,140d], K. Maj[84a], O. Majersky[28a], S. Majewski[132], Y. Makida[82], N. Makovec[65], B. Malaescu[136], Pa. Malecki[85], V.P. Maleev[138], F. Malek[58], U. Mallik[78], D. Malon[6], C. Malone[32], S. Maltezos[10], S. Malyukov[80], J. Mamuzic[174], G. Mancini[51], I. Mandić[92], L. Manhaes de Andrade Filho[81a], I.M. Maniatis[162], J. Manjarres Ramos[48], K.H. Mankinen[97], A. Mann[114], A. Manousos[77], B. Mansoulie[145], I. Manthos[162], S. Manzoni[120], A. Marantis[162], G. Marceca[30], L. Marchese[135], G. Marchiori[136], M. Marcisovsky[141], L. Marcoccia[74a,74b], C. Marcon[97], C.A. Marin Tobon[36], M. Marjanovic[129], Z. Marshall[18], M.U.F. Martensson[172], S. Marti-Garcia[174], C.B. Martin[127], T.A. Martin[178], V.J. Martin[50], B. Martin dit Latour[17], L. Martinelli[75a,75b], M. Martinez[14,z], V.I. Martinez Outschoorn[103], S. Martin-Haugh[144], V.S. Martoiu[27b], A.C. Martyniuk[95], A. Marzin[36], S.R. Maschek[115], L. Masetti[100], T. Mashimo[163], R. Mashinistov[111], J. Masik[101], A.L. Maslennikov[122b,122a], L. Massa[74a,74b], P. Massarotti[70a,70b], P. Mastrandrea[72a,72b], A. Mastroberardino[41b,41a], T. Masubuchi[163], D. Matakias[10], A. Matic[114], N. Matsuzawa[163], P. Mättig[24], J. Maurer[27b], B. Maček[92], D.A. Maximov[122b,122a], R. Mazini[158], I. Maznas[162], S.M. Mazza[146], S.P. Mc Kee[106], T.G. McCarthy[115], W.P. McCormack[18], E.F. McDonald[105], J.A. Mcfayden[36], G. Mchedlidze[159b], M.A. McKay[42], K.D. McLean[176], S.J. McMahon[144], P.C. McNamara[105], C.J. McNicol[178], R.A. McPherson[176,ae], J.E. Mdhluli[33d], Z.A. Meadows[103], S. Meehan[36], T. Megy[52], S. Mehlhase[114], A. Mehta[91], T. Meideck[58], B. Meirose[43], D. Melini[160], B.R. Mellado Garcia[33d], J.D. Mellenthin[53], M. Melo[28a], F. Meloni[46], A. Melzer[24], S.B. Menary[101], E.D. Mendes Gouveia[140a,140e], L. Meng[36], X.T. Meng[106], S. Menke[115], E. Meoni[41b,41a], S. Mergelmeyer[19], S.A.M. Merkt[139], C. Merlassino[135], P. Mermod[54], L. Merola[70a,70b], C. Meroni[69a], G. Merz[106], O. Meshkov[113,111], J.K.R. Meshreki[151], A. Messina[73a,73b], J. Metcalfe[6], A.S. Mete[6], C. Meyer[66], J-P. Meyer[145], H. Meyer Zu Theenhausen[61a], F. Miano[156], M. Michetti[19], R.P. Middleton[144], L. Mijović[50], G. Mikenberg[180], M. Mikestikova[141], M. Mikuž[92], H. Mildner[149], M. Milesi[105], A. Milic[167], D.A. Millar[93], D.W. Miller[37], A. Milov[180], D.A. Milstead[45a,45b], R.A. Mina[153], A.A. Minaenko[123],

M. Miñano Moya[174], I.A. Minashvili[159b], A.I. Mincer[125], B. Mindur[84a], M. Mineev[80], Y. Minegishi[163], L.M. Mir[14], A. Mirto[68a,68b], K.P. Mistry[137], T. Mitani[179], J. Mitrevski[114], V.A. Mitsou[174], M. Mittal[60c], O. Miu[167], A. Miucci[20], P.S. Miyagawa[149], A. Mizukami[82], J.U. Mjörnmark[97], T. Mkrtchyan[61a], M. Mlynarikova[143], T. Moa[45a,45b], K. Mochizuki[110], P. Mogg[52], S. Mohapatra[39], R. Moles-Valls[24], M.C. Mondragon[107], K. Mönig[46], J. Monk[40], E. Monnier[102], A. Montalbano[152], J. Montejo Berlingen[36], M. Montella[95], F. Monticelli[89], S. Monzani[69a], N. Morange[65], D. Moreno[22], M. Moreno Llácer[174], C. Moreno Martinez[14], P. Morettini[55b], M. Morgenstern[120], S. Morgenstern[48], D. Mori[152], M. Morii[59], M. Morinaga[179], V. Morisbak[134], A.K. Morley[36], G. Mornacchi[36], A.P. Morris[95], L. Morvaj[155], P. Moschovakos[36], B. Moser[120], M. Mosidze[159b], T. Moskalets[145], H.J. Moss[149], J. Moss[31,m], E.J.W. Moyse[103], S. Muanza[102], J. Mueller[139], R.S.P. Mueller[114], D. Muenstermann[90], G.A. Mullier[97], D.P. Mungo[69a,69b], J.L. Munoz Martinez[14], F.J. Munoz Sanchez[101], P. Murin[28b], W.J. Murray[178,144], A. Murrone[69a,69b], M. Muškinja[18], C. Mwewa[33a], A.G. Myagkov[123,ak], A.A. Myers[139], J. Myers[132], M. Myska[142], B.P. Nachman[18], O. Nackenhorst[47], A.Nag Nag[48], K. Nagai[135], K. Nagano[82], Y. Nagasaka[62], J.L. Nagle[29], E. Nagy[102], A.M. Nairz[36], Y. Nakahama[117], K. Nakamura[82], T. Nakamura[163], I. Nakano[128], H. Nanjo[133], F. Napolitano[61a], R.F. Naranjo Garcia[46], R. Narayan[42], I. Naryshkin[138], T. Naumann[46], G. Navarro[22], P.Y. Nechaeva[111], F. Nechansky[46], T.J. Neep[21], A. Negri[71a,71b], M. Negrini[23b], C. Nellist[53], M.E. Nelson[45a,45b], S. Nemecek[141], P. Nemethy[125], M. Nessi[36,d], M.S. Neubauer[173], F. Neuhaus[100], M. Neumann[182], R. Newhouse[175], P.R. Newman[21], C.W. Ng[139], Y.S. Ng[19], Y.W.Y. Ng[171], B. Ngair[35e], H.D.N. Nguyen[102], T. Nguyen Manh[110], E. Nibigira[38], R.B. Nickerson[135], R. Nicolaidou[145], D.S. Nielsen[40], J. Nielsen[146], N. Nikiforou[11], V. Nikolaenko[123,ak], I. Nikolic-Audit[136], K. Nikolopoulos[21], P. Nilsson[29], H.R. Nindhito[54], Y. Ninomiya[82], A. Nisati[73a], N. Nishu[60c], R. Nisius[115], I. Nitsche[47], T. Nitta[179], T. Nobe[163], Y. Noguchi[86], I. Nomidis[136], M.A. Nomura[29], M. Nordberg[36], N. Norjoharuddeen[135], T. Novak[92], O. Novgorodova[48], R. Novotny[142], L. Nozka[131], K. Ntekas[171], E. Nurse[95], F.G. Oakham[34,ar], H. Oberlack[115], J. Ocariz[136], A. Ochi[83], I. Ochoa[39], J.P. Ochoa-Ricoux[147a], K. O'Connor[26], S. Oda[88], S. Odaka[82], S. Oerdek[53], A. Ogrodnik[84a], A. Oh[101], S.H. Oh[49], C.C. Ohm[154], H. Oide[165], M.L. Ojeda[167], H. Okawa[169], Y. Okazaki[86], M.W. O'Keefe[91], Y. Okumura[163], T. Okuyama[82], A. Olariu[27b], L.F. Oleiro Seabra[140a], S.A. Olivares Pino[147a], D. Oliveira Damazio[29], J.L. Oliver[1], M.J.R. Olsson[171], A. Olszewski[85], J. Olszowska[85], D.C. O'Neil[152], A.P. O'neill[135], A. Onofre[140a,140e], P.U.E. Onyisi[11], H. Oppen[134], M.J. Oreglia[37], G.E. Orellana[89], D. Orestano[75a,75b], N. Orlando[14], R.S. Orr[167], V. O'Shea[57], R. Ospanov[60a], G. Otero y Garzon[30], H. Otono[88], P.S. Ott[61a], M. Ouchrif[35d], J. Ouellette[29], F. Ould-Saada[134], A. Ouraou[145], Q. Ouyang[15a], M. Owen[57], R.E. Owen[21], V.E. Ozcan[12c], N. Ozturk[8], J. Pacalt[131], H.A. Pacey[32], K. Pachal[49], A. Pacheco Pages[14], C. Padilla Aranda[14], S. Pagan Griso[18], M. Paganini[183], G. Palacino[66], S. Palazzo[50], S. Palestini[36], M. Palka[84b], D. Pallin[38], I. Panagoulias[10], C.E. Pandini[36], J.G. Panduro Vazquez[94], P. Pani[46], G. Panizzo[67a,67c], L. Paolozzi[54], C. Papadatos[110], K. Papageorgiou[9,g], S. Parajuli[43], A. Paramonov[6], D. Paredes Hernandez[63b], S.R. Paredes Saenz[135], B. Parida[166], T.H. Park[167], A.J. Parker[31], M.A. Parker[32], F. Parodi[55b,55a], E.W. Parrish[121], J.A. Parsons[39], U. Parzefall[52], L. Pascual Dominguez[136], V.R. Pascuzzi[167], J.M.P. Pasner[146], F. Pasquali[120], E. Pasqualucci[73a], S. Passaggio[55b], F. Pastore[94], P. Pasuwan[45a,45b], S. Pataraia[100], J.R. Pater[101], A. Pathak[181,i], J. Patton[91], T. Pauly[36], J. Pearkes[153], B. Pearson[115], M. Pedersen[134], L. Pedraza Diaz[119], R. Pedro[140a], T. Peiffer[53], S.V. Peleganchuk[122b,122a], O. Penc[141], H. Peng[60a], B.S. Peralva[81a], M.M. Perego[65], A.P. Pereira Peixoto[140a], D.V. Perepelitsa[29], F. Peri[19], L. Perini[69a,69b], H. Pernegger[36], S. Perrella[140a], A. Perrevoort[120], K. Peters[46], R.F.Y. Peters[101], B.A. Petersen[36], T.C. Petersen[40], E. Petit[102], A. Petridis[1], C. Petridou[162], P. Petroff[65], M. Petrov[135], F. Petrucci[75a,75b], M. Pettee[183], N.E. Pettersson[103], K. Petukhova[143], A. Peyaud[145], R. Pezoa[147c], L. Pezzotti[71a,71b], T. Pham[105], F.H. Phillips[107], P.W. Phillips[144], M.W. Phipps[173], G. Piacquadio[155], E. Pianori[18], A. Picazio[103], R.H. Pickles[101], R. Piegaia[30], D. Pietreanu[27b], J.E. Pilcher[37], A.D. Pilkington[101], M. Pinamonti[67a,67c], J.L. Pinfold[3], M. Pitt[161], L. Pizzimento[74a,74b], M.-A. Pleier[29],

V. Pleskot[143], E. Plotnikova[80], P. Podberezko[122b,122a], R. Poettgen[97], R. Poggi[54], L. Poggioli[65], I. Pogrebnyak[107], D. Pohl[24], I. Pokharel[53], G. Polesello[71a], A. Poley[18], A. Policicchio[73a,73b], R. Polifka[143], A. Polini[23b], C.S. Pollard[46], V. Polychronakos[29], D. Ponomarenko[112], L. Pontecorvo[36], S. Popa[27a], G.A. Popeneciu[27d], L. Portales[5], D.M. Portillo Quintero[58], S. Pospisil[142], K. Potamianos[46], I.N. Potrap[80], C.J. Potter[32], H. Potti[11], T. Poulsen[97], J. Poveda[36], T.D. Powell[149], G. Pownall[46], M.E. Pozo Astigarraga[36], P. Pralavorio[102], S. Prell[79], D. Price[101], M. Primavera[68a], S. Prince[104], M.L. Proffitt[148], N. Proklova[112], K. Prokofiev[63c], F. Prokoshin[80], S. Protopopescu[29], J. Proudfoot[6], M. Przybycien[84a], D. Pudzha[138], A. Puri[173], P. Puzo[65], J. Qian[106], Y. Qin[101], A. Quadt[53], M. Queitsch-Maitland[36], A. Qureshi[1], M. Racko[28a], F. Ragusa[69a,69b], G. Rahal[98], J.A. Raine[54], S. Rajagopalan[29], A. Ramirez Morales[93], K. Ran[15a,15d], T. Rashid[65], S. Raspopov[5], D.M. Rauch[46], F. Rauscher[114], S. Rave[100], B. Ravina[149], I. Ravinovich[180], J.H. Rawling[101], M. Raymond[36], A.L. Read[134], N.P. Readioff[58], M. Reale[68a,68b], D.M. Rebuzzi[71a,71b], A. Redelbach[177], G. Redlinger[29], K. Reeves[43], L. Rehnisch[19], J. Reichert[137], D. Reikher[161], A. Reiss[100], A. Rej[151], C. Rembser[36], A. Renardi[46], M. Renda[27b], M. Rescigno[73a], S. Resconi[69a], E.D. Resseguie[137], S. Rettie[175], B. Reynolds[127], E. Reynolds[21], O.L. Rezanova[122b,122a], P. Reznicek[143], E. Ricci[76a,76b], R. Richter[115], S. Richter[46], E. Richter-Was[84b], O. Ricken[24], M. Ridel[136], P. Rieck[115], O. Rifki[46], M. Rijssenbeek[155], A. Rimoldi[71a,71b], M. Rimoldi[46], L. Rinaldi[23b], G. Ripellino[154], I. Riu[14], J.C. Rivera Vergara[176], F. Rizatdinova[130], E. Rizvi[93], C. Rizzi[36], R.T. Roberts[101], S.H. Robertson[104,ae], M. Robin[46], D. Robinson[32], J.E.M. Robinson[46], C.M. Robles Gajardo[147c], M. Robles Manzano[100], A. Robson[57], A. Rocchi[74a,74b], E. Rocco[100], C. Roda[72a,72b], S. Rodriguez Bosca[174], A. Rodriguez Perez[14], D. Rodriguez Rodriguez[174], A.M. Rodríguez Vera[168b], S. Roe[36], O. Røhne[134], R. Röhrig[115], R.A. Rojas[147c], B. Roland[52], C.P.A. Roland[66], J. Roloff[29], A. Romaniouk[112], M. Romano[23b,23a], N. Rompotis[91], M. Ronzani[125], L. Roos[136], S. Rosati[73a], G. Rosin[103], B.J. Rosser[137], E. Rossi[46], E. Rossi[75a,75b], E. Rossi[70a,70b], L.P. Rossi[55b], L. Rossini[69a,69b], R. Rosten[14], M. Rotaru[27b], J. Rothberg[148], B. Rottler[52], D. Rousseau[65], G. Rovelli[71a,71b], A. Roy[11], D. Roy[33d], A. Rozanov[102], Y. Rozen[160], X. Ruan[33d], F. Rühr[52], A. Ruiz-Martinez[174], A. Rummler[36], Z. Rurikova[52], N.A. Rusakovich[80], H.L. Russell[104], L. Rustige[38,47], J.P. Rutherfoord[7], E.M. Rüttinger[149], M. Rybar[39], G. Rybkin[65], E.B. Rye[134], A. Ryzhov[123], J.A. Sabater Iglesias[46], P. Sabatini[53], G. Sabato[120], S. Sacerdoti[65], H.F-W. Sadrozinski[146], R. Sadykov[80], F. Safai Tehrani[73a], B. Safarzadeh Samani[156], M. Safdari[153], P. Saha[121], S. Saha[104], M. Sahinsoy[61a], A. Sahu[182], M. Saimpert[46], M. Saito[163], T. Saito[163], H. Sakamoto[163], A. Sakharov[125,aj], D. Salamani[54], G. Salamanna[75a,75b], J.E. Salazar Loyola[147c], A. Salnikov[153], J. Salt[174], D. Salvatore[41b,41a], F. Salvatore[156], A. Salvucci[63a,63b,63c], A. Salzburger[36], J. Samarati[36], D. Sammel[52], D. Sampsonidis[162], D. Sampsonidou[162], J. Sánchez[174], A. Sanchez Pineda[67a,36,67c], H. Sandaker[134], C.O. Sander[46], I.G. Sanderswood[90], M. Sandhoff[182], C. Sandoval[22], D.P.C. Sankey[144], M. Sannino[55b,55a], Y. Sano[117], A. Sansoni[51], C. Santoni[38], H. Santos[140a,140b], S.N. Santpur[18], A. Santra[174], A. Sapronov[80], J.G. Saraiva[140a,140d], O. Sasaki[82], K. Sato[169], F. Sauerburger[52], E. Sauvan[5], P. Savard[167,ar], R. Sawada[163], C. Sawyer[144], L. Sawyer[96,ai], C. Sbarra[23b], A. Sbrizzi[23a], T. Scanlon[95], J. Schaarschmidt[148], P. Schacht[115], B.M. Schachtner[114], D. Schaefer[37], L. Schaefer[137], J. Schaeffer[100], S. Schaepe[36], U. Schäfer[100], A.C. Schaffer[65], D. Schaile[114], R.D. Schamberger[155], N. Scharmberg[101], V.A. Schegelsky[138], D. Scheirich[143], F. Schenck[19], M. Schernau[171], C. Schiavi[55b,55a], S. Schier[146], L.K. Schildgen[24], Z.M. Schillaci[26], E.J. Schioppa[36], M. Schioppa[41b,41a], K.E. Schleicher[52], S. Schlenker[36], K.R. Schmidt-Sommerfeld[115], K. Schmieden[36], C. Schmitt[100], S. Schmitt[46], S. Schmitz[100], J.C. Schmoeckel[46], U. Schnoor[52], L. Schoeffel[145], A. Schoening[61b], P.G. Scholer[52], E. Schopf[135], M. Schott[100], J.F.P. Schouwenberg[119], J. Schovancova[36], S. Schramm[54], F. Schroeder[182], A. Schulte[100], H-C. Schultz-Coulon[61a], M. Schumacher[52], B.A. Schumm[146], Ph. Schune[145], A. Schwartzman[153], T.A. Schwarz[106], Ph. Schwemling[145], R. Schwienhorst[107], A. Sciandra[146], G. Sciolla[26], M. Scodeggio[46], M. Scornajenghi[41b,41a], F. Scuri[72a], F. Scutti[105], L.M. Scyboz[115], C.D. Sebastiani[73a,73b], P. Seema[19], S.C. Seidel[118], A. Seiden[146],

B.D. Seidlitz[29], T. Seiss[37], J.M. Seixas[81b], G. Sekhniaidze[70a], K. Sekhon[106], S.J. Sekula[42], N. Semprini-Cesari[23b,23a], S. Sen[49], C. Serfon[77], L. Serin[65], L. Serkin[67a,67b], M. Sessa[60a], H. Severini[129], S. Sevova[153], T. Šfiligoj[92], F. Sforza[55b,55a], A. Sfyrla[54], E. Shabalina[53], J.D. Shahinian[146], N.W. Shaikh[45a,45b], D. Shaked Renous[180], L.Y. Shan[15a], J.T. Shank[25], M. Shapiro[18], A. Sharma[135], A.S. Sharma[1], P.B. Shatalov[124], K. Shaw[156], S.M. Shaw[101], M. Shehade[180], Y. Shen[129], A.D. Sherman[25], P. Sherwood[95], L. Shi[158], S. Shimizu[82], C.O. Shimmin[183], Y. Shimogama[179], M. Shimojima[116], I.P.J. Shipsey[135], S. Shirabe[165], M. Shiyakova[80,ac], J. Shlomi[180], A. Shmeleva[111], M.J. Shochet[37], J. Shojaii[105], D.R. Shope[129], S. Shrestha[127], E.M. Shrif[33d], E. Shulga[180], P. Sicho[141], A.M. Sickles[173], P.E. Sidebo[154], E. Sideras Haddad[33d], O. Sidiropoulou[36], A. Sidoti[23b,23a], F. Siegert[48], Dj. Sijacki[16], M.Jr. Silva[181], M.V. Silva Oliveira[81a], S.B. Silverstein[45a], S. Simion[65], R. Simoniello[100], S. Simsek[12b], P. Sinervo[167], V. Sinetckii[113], N.B. Sinev[132], S. Singh[152], M. Sioli[23b,23a], I. Siral[132], S.Yu. Sivoklokov[113], J. Sjölin[45a,45b], E. Skorda[97], P. Skubic[129], M. Slawinska[85], K. Sliwa[170], R. Slovak[143], V. Smakhtin[180], B.H. Smart[144], J. Smiesko[28a], N. Smirnov[112], S.Yu. Smirnov[112], Y. Smirnov[112], L.N. Smirnova[113,u], O. Smirnova[97], J.W. Smith[53], M. Smizanska[90], K. Smolek[142], A. Smykiewicz[85], A.A. Snesarev[111], H.L. Snoek[120], I.M. Snyder[132], S. Snyder[29], R. Sobie[176,ae], A. Soffer[161], A. Søgaard[50], F. Sohns[53], C.A. Solans Sanchez[36], E.Yu. Soldatov[112], U. Soldevila[174], A.A. Solodkov[123], A. Soloshenko[80], O.V. Solovyanov[123], V. Solovyev[138], P. Sommer[149], H. Son[170], W. Song[144], W.Y. Song[168b], A. Sopczak[142], A.L. Sopio[95], F. Sopkova[28b], C.L. Sotiropoulou[72a,72b], S. Sottocornola[71a,71b], R. Soualah[67a,67c,f], A.M. Soukharev[122b,122a], D. South[46], S. Spagnolo[68a,68b], M. Spalla[115], M. Spangenberg[178], F. Spanò[94], D. Sperlich[52], T.M. Spieker[61a], G. Spigo[36], M. Spina[156], D.P. Spiteri[57], M. Spousta[143], A. Stabile[69a,69b], B.L. Stamas[121], R. Stamen[61a], M. Stamenkovic[120], E. Stanecka[85], B. Stanislaus[135], M.M. Stanitzki[46], M. Stankaityte[135], B. Stapf[120], E.A. Starchenko[123], G.H. Stark[146], J. Stark[58], S.H. Stark[40], P. Staroba[141], P. Starovoitov[61a], S. Stärz[104], R. Staszewski[85], G. Stavropoulos[44], M. Stegler[46], P. Steinberg[29], A.L. Steinhebel[132], B. Stelzer[152], H.J. Stelzer[139], O. Stelzer-Chilton[168a], H. Stenzel[56], T.J. Stevenson[156], G.A. Stewart[36], M.C. Stockton[36], G. Stoicea[27b], M. Stolarski[140a], S. Stonjek[115], A. Straessner[48], J. Strandberg[154], S. Strandberg[45a,45b], M. Strauss[129], P. Strizenec[28b], R. Ströhmer[177], D.M. Strom[132], R. Stroynowski[42], A. Strubig[50], S.A. Stucci[29], B. Stugu[17], J. Stupak[129], N.A. Styles[46], D. Su[153], W. Su[60c], S. Suchek[61a], V.V. Sulin[111], M.J. Sullivan[91], D.M.S. Sultan[54], S. Sultansoy[4c], T. Sumida[86], S. Sun[106], X. Sun[3], K. Suruliz[156], C.J.E. Suster[157], M.R. Sutton[156], S. Suzuki[82], M. Svatos[141], M. Swiatlowski[37], S.P. Swift[2], T. Swirski[177], A. Sydorenko[100], I. Sykora[28a], M. Sykora[143], T. Sykora[143], D. Ta[100], K. Tackmann[46,aa], J. Taenzer[161], A. Taffard[171], R. Tafirout[168a], H. Takai[29], R. Takashima[87], K. Takeda[83], T. Takeshita[150], E.P. Takeva[50], Y. Takubo[82], M. Talby[102], A.A. Talyshev[122b,122a], N.M. Tamir[161], J. Tanaka[163], M. Tanaka[165], R. Tanaka[65], S. Tapia Araya[173], S. Tapprogge[100], A. Tarek Abouelfadl Mohamed[136], S. Tarem[160], K. Tariq[60b], G. Tarna[27b,c], G.F. Tartarelli[69a], P. Tas[143], M. Tasevsky[141], T. Tashiro[86], E. Tassi[41b,41a], A. Tavares Delgado[140a], Y. Tayalati[35e], A.J. Taylor[50], G.N. Taylor[105], W. Taylor[168b], A.S. Tee[90], R. Teixeira De Lima[153], P. Teixeira-Dias[94], H. Ten Kate[36], J.J. Teoh[120], S. Terada[82], K. Terashi[163], J. Terron[99], S. Terzo[14], M. Testa[51], R.J. Teuscher[167,ae], S.J. Thais[183], T. Theveneaux-Pelzer[46], F. Thiele[40], D.W. Thomas[94], J.O. Thomas[42], J.P. Thomas[21], P.D. Thompson[21], L.A. Thomsen[183], E. Thomson[137], E.J. Thorpe[93], R.E. Ticse Torres[53], V.O. Tikhomirov[111,al], Yu.A. Tikhonov[122b,122a], S. Timoshenko[112], P. Tipton[183], S. Tisserant[102], K. Todome[23b,23a], S. Todorova-Nova[5], S. Todt[48], J. Tojo[88], S. Tokár[28a], K. Tokushuku[82], E. Tolley[127], K.G. Tomiwa[33d], M. Tomoto[117], L. Tompkins[153,p], B. Tong[59], P. Tornambe[103], E. Torrence[132], H. Torres[48], E. Torró Pastor[148], C. Tosciri[135], J. Toth[102,ad], D.R. Tovey[149], A. Traeet[17], C.J. Treado[125], T. Trefzger[177], F. Tresoldi[156], A. Tricoli[29], I.M. Trigger[168a], S. Trincaz-Duvoid[136], D.T. Trischuk[175], W. Trischuk[167], B. Trocmé[58], A. Trofymov[145], C. Troncon[69a], M. Trovatelli[176], F. Trovato[156], L. Truong[33b], M. Trzebinski[85], A. Trzupek[85], F. Tsai[46], J.C-L. Tseng[135], P.V. Tsiareshka[108,ah], A. Tsirigotis[162,x], V. Tsiskaridze[155], E.G. Tskhadadze[159a], M. Tsopoulou[162], I.I. Tsukerman[124], V. Tsulaia[18], S. Tsuno[82],

D. Tsybychev[155], Y. Tu[63b], A. Tudorache[27b], V. Tudorache[27b], T.T. Tulbure[27a], A.N. Tuna[59], S. Turchikhin[80], D. Turgeman[180], I. Turk Cakir[4b,v], R.J. Turner[21], R.T. Turra[69a], P.M. Tuts[39], S. Tzamarias[162], E. Tzovara[100], G. Ucchielli[47], K. Uchida[163], I. Ueda[82], F. Ukegawa[169], G. Unal[36], A. Undrus[29], G. Unel[171], F.C. Ungaro[105], Y. Unno[82], K. Uno[163], J. Urban[28b], P. Urquijo[105], G. Usai[8], Z. Uysal[12d], V. Vacek[142], B. Vachon[104], K.O.H. Vadla[134], A. Vaidya[95], C. Valderanis[114], E. Valdes Santurio[45a,45b], M. Valente[54], S. Valentinetti[23b,23a], A. Valero[174], L. Valéry[46], R.A. Vallance[21], A. Vallier[36], J.A. Valls Ferrer[174], T.R. Van Daalen[14], P. Van Gemmeren[6], I. Van Vulpen[120], M. Vanadia[74a,74b], W. Vandelli[36], M. Vandenbroucke[145], E.R. Vandewall[130], A. Vaniachine[166], D. Vannicola[73a,73b], R. Vari[73a], E.W. Varnes[7], C. Varni[55b,55a], T. Varol[158], D. Varouchas[65], K.E. Varvell[157], M.E. Vasile[27b], G.A. Vasquez[176], F. Vazeille[38], D. Vazquez Furelos[14], T. Vazquez Schroeder[36], J. Veatch[53], V. Vecchio[75a,75b], M.J. Veen[120], L.M. Veloce[167], F. Veloso[140a,140c], S. Veneziano[73a], A. Ventura[68a,68b], N. Venturi[36], A. Verbytskyi[115], V. Vercesi[71a], M. Verducci[72a,72b], C.M. Vergel Infante[79], C. Vergis[24], W. Verkerke[120], A.T. Vermeulen[120], J.C. Vermeulen[120], M.C. Vetterli[152,ar], N. Viaux Maira[147c], M. Vicente Barreto Pinto[54], T. Vickey[149], O.E. Vickey Boeriu[149], G.H.A. Viehhauser[135], L. Vigani[61b], M. Villa[23b,23a], M. Villaplana Perez[3], E. Vilucchi[51], M.G. Vincter[34], G.S. Virdee[21], A. Vishwakarma[46], C. Vittori[23b,23a], I. Vivarelli[156], M. Vogel[182], P. Vokac[142], S.E. von Buddenbrock[33d], E. Von Toerne[24], V. Vorobel[143], K. Vorobev[112], M. Vos[174], J.H. Vossebeld[91], M. Vozak[101], N. Vranjes[16], M. Vranjes Milosavljevic[16], V. Vrba[142], M. Vreeswijk[120], R. Vuillermet[36], I. Vukotic[37], P. Wagner[24], W. Wagner[182], J. Wagner-Kuhr[114], S. Wahdan[182], H. Wahlberg[89], V.M. Walbrecht[115], J. Walder[90], R. Walker[114], S.D. Walker[94], W. Walkowiak[151], V. Wallangen[45a,45b], A.M. Wang[59], A.Z. Wang[181], C. Wang[60c], F. Wang[181], H. Wang[18], H. Wang[3], J. Wang[63a], J. Wang[61b], P. Wang[42], Q. Wang[129], R.-J. Wang[100], R. Wang[60a], R. Wang[6], S.M. Wang[158], W.T. Wang[60a], W. Wang[15c], W.X. Wang[60a], Y. Wang[60a], Z. Wang[60c], C. Wanotayaroj[46], A. Warburton[104], C.P. Ward[32], D.R. Wardrope[95], N. Warrack[57], A. Washbrook[50], A.T. Watson[21], M.F. Watson[21], G. Watts[148], B.M. Waugh[95], A.F. Webb[11], S. Webb[100], C. Weber[183], M.S. Weber[20], S.A. Weber[34], S.M. Weber[61a], A.R. Weidberg[135], J. Weingarten[47], M. Weirich[100], C. Weiser[52], P.S. Wells[36], T. Wenaus[29], T. Wengler[36], S. Wenig[36], N. Wermes[24], M.D. Werner[79], M. Wessels[61a], T.D. Weston[20], K. Whalen[132], N.L. Whallon[148], A.M. Wharton[90], A.S. White[106], A. White[8], M.J. White[1], D. Whiteson[171], B.W. Whitmore[90], W. Wiedenmann[181], C. Wiel[48], M. Wielers[144], N. Wieseotte[100], C. Wiglesworth[40], L.A.M. Wiik-Fuchs[52], H.G. Wilkens[36], L.J. Wilkins[94], H.H. Williams[137], S. Williams[32], C. Willis[107], S. Willocq[103], J.A. Wilson[21], I. Wingerter-Seez[5], E. Winkels[156], F. Winklmeier[132], O.J. Winston[156], B.T. Winter[52], M. Wittgen[153], M. Wobisch[96], A. Wolf[100], T.M.H. Wolf[120], R. Wolff[102], R.W. Wölker[135], J. Wollrath[52], M.W. Wolter[85], H. Wolters[140a,140c], V.W.S. Wong[175], N.L. Woods[146], S.D. Worm[21], B.K. Wosiek[85], K.W. Woźniak[85], K. Wraight[57], S.L. Wu[181], X. Wu[54], Y. Wu[60a], T.R. Wyatt[101], B.M. Wynne[50], S. Xella[40], Z. Xi[106], L. Xia[178], X. Xiao[106], I. Xiotidis[156], D. Xu[15a], H. Xu[60a], H. Xu[60a], L. Xu[29], T. Xu[145], W. Xu[106], Z. Xu[60b], Z. Xu[153], B. Yabsley[157], S. Yacoob[33a], K. Yajima[133], D.P. Yallup[95], N. Yamaguchi[88], Y. Yamaguchi[165], A. Yamamoto[82], M. Yamatani[163], T. Yamazaki[163], Y. Yamazaki[83], Z. Yan[25], H.J. Yang[60c,60d], H.T. Yang[18], S. Yang[60a], X. Yang[60b,58], Y. Yang[163], W-M. Yao[18], Y.C. Yap[46], Y. Yasu[82], E. Yatsenko[60c,60d], H. Ye[15c], J. Ye[42], S. Ye[29], I. Yeletskikh[80], M.R. Yexley[90], E. Yigitbasi[25], K. Yorita[179], K. Yoshihara[137], C.J.S. Young[36], C. Young[153], J. Yu[79], R. Yuan[60b,h], X. Yue[61a], S.P.Y. Yuen[24], M. Zaazoua[35e], B. Zabinski[85], G. Zacharis[10], E. Zaffaroni[54], J. Zahreddine[136], A.M. Zaitsev[123,ak], T. Zakareishvili[159b], N. Zakharchuk[34], S. Zambito[59], D. Zanzi[36], D.R. Zaripovas[57], S.V. Zeißner[47], C. Zeitnitz[182], G. Zemaityte[135], J.C. Zeng[173], O. Zenin[123], T. Ženiš[28a], D. Zerwas[65], M. Zgubič[135], B. Zhang[15c], D.F. Zhang[15b], G. Zhang[15b], H. Zhang[15c], J. Zhang[6], L. Zhang[15c], L. Zhang[60a], M. Zhang[173], R. Zhang[181], S. Zhang[106], X. Zhang[60b], Y. Zhang[15a,15d], Z. Zhang[63a], Z. Zhang[65], P. Zhao[49], Y. Zhao[60b], Z. Zhao[60a], A. Zhemchugov[80], Z. Zheng[106], D. Zhong[173], B. Zhou[106], C. Zhou[181], M.S. Zhou[15a,15d], M. Zhou[155], N. Zhou[60c], Y. Zhou[7], C.G. Zhu[60b], C. Zhu[15a,15d], H.L. Zhu[60a], H. Zhu[15a], J. Zhu[106], Y. Zhu[60a],

X. Zhuang[15a], K. Zhukov[111], V. Zhulanov[122b,122a], D. Zieminska[66], N.I. Zimine[80], S. Zimmermann[52], Z. Zinonos[115], M. Ziolkowski[151], L. Živković[16], G. Zobernig[181], A. Zoccoli[23b,23a], K. Zoch[53], T.G. Zorbas[149], R. Zou[37], L. Zwalinski[36].

[1]Department of Physics, University of Adelaide, Adelaide; Australia.
[2]Physics Department, SUNY Albany, Albany NY; United States of America.
[3]Department of Physics, University of Alberta, Edmonton AB; Canada.
[4(a)]Department of Physics, Ankara University, Ankara;[(b)]Istanbul Aydin University, Istanbul;[(c)]Division of Physics, TOBB University of Economics and Technology, Ankara; Turkey.
[5]LAPP, Université Grenoble Alpes, Université Savoie Mont Blanc, CNRS/IN2P3, Annecy; France.
[6]High Energy Physics Division, Argonne National Laboratory, Argonne IL; United States of America.
[7]Department of Physics, University of Arizona, Tucson AZ; United States of America.
[8]Department of Physics, University of Texas at Arlington, Arlington TX; United States of America.
[9]Physics Department, National and Kapodistrian University of Athens, Athens; Greece.
[10]Physics Department, National Technical University of Athens, Zografou; Greece.
[11]Department of Physics, University of Texas at Austin, Austin TX; United States of America.
[12(a)]Bahcesehir University, Faculty of Engineering and Natural Sciences, Istanbul;[(b)]Istanbul Bilgi University, Faculty of Engineering and Natural Sciences, Istanbul;[(c)]Department of Physics, Bogazici University, Istanbul;[(d)]Department of Physics Engineering, Gaziantep University, Gaziantep; Turkey.
[13]Institute of Physics, Azerbaijan Academy of Sciences, Baku; Azerbaijan.
[14]Institut de Física d'Altes Energies (IFAE), Barcelona Institute of Science and Technology, Barcelona; Spain.
[15(a)]Institute of High Energy Physics, Chinese Academy of Sciences, Beijing;[(b)]Physics Department, Tsinghua University, Beijing;[(c)]Department of Physics, Nanjing University, Nanjing;[(d)]University of Chinese Academy of Science (UCAS), Beijing; China.
[16]Institute of Physics, University of Belgrade, Belgrade; Serbia.
[17]Department for Physics and Technology, University of Bergen, Bergen; Norway.
[18]Physics Division, Lawrence Berkeley National Laboratory and University of California, Berkeley CA; United States of America.
[19]Institut für Physik, Humboldt Universität zu Berlin, Berlin; Germany.
[20]Albert Einstein Center for Fundamental Physics and Laboratory for High Energy Physics, University of Bern, Bern; Switzerland.
[21]School of Physics and Astronomy, University of Birmingham, Birmingham; United Kingdom.
[22]Facultad de Ciencias y Centro de Investigaciónes, Universidad Antonio Nariño, Bogota; Colombia.
[23(a)]INFN Bologna and Universita' di Bologna, Dipartimento di Fisica;[(b)]INFN Sezione di Bologna; Italy.
[24]Physikalisches Institut, Universität Bonn, Bonn; Germany.
[25]Department of Physics, Boston University, Boston MA; United States of America.
[26]Department of Physics, Brandeis University, Waltham MA; United States of America.
[27(a)]Transilvania University of Brasov, Brasov;[(b)]Horia Hulubei National Institute of Physics and Nuclear Engineering, Bucharest;[(c)]Department of Physics, Alexandru Ioan Cuza University of Iasi, Iasi;[(d)]National Institute for Research and Development of Isotopic and Molecular Technologies, Physics Department, Cluj-Napoca;[(e)]University Politehnica Bucharest, Bucharest;[(f)]West University in Timisoara, Timisoara; Romania.
[28(a)]Faculty of Mathematics, Physics and Informatics, Comenius University, Bratislava;[(b)]Department of Subnuclear Physics, Institute of Experimental Physics of the Slovak Academy of Sciences, Kosice; Slovak Republic.
[29]Physics Department, Brookhaven National Laboratory, Upton NY; United States of America.

[30]Departamento de Física, Universidad de Buenos Aires, Buenos Aires; Argentina.
[31]California State University, CA; United States of America.
[32]Cavendish Laboratory, University of Cambridge, Cambridge; United Kingdom.
[33(a)]Department of Physics, University of Cape Town, Cape Town;[(b)]Department of Mechanical Engineering Science, University of Johannesburg, Johannesburg;[(c)]University of South Africa, Department of Physics, Pretoria;[(d)]School of Physics, University of the Witwatersrand, Johannesburg; South Africa.
[34]Department of Physics, Carleton University, Ottawa ON; Canada.
[35(a)]Faculté des Sciences Ain Chock, Réseau Universitaire de Physique des Hautes Energies - Université Hassan II, Casablanca;[(b)]Faculté des Sciences, Université Ibn-Tofail, Kénitra;[(c)]Faculté des Sciences Semlalia, Université Cadi Ayyad, LPHEA-Marrakech;[(d)]Faculté des Sciences, Université Mohamed Premier and LPTPM, Oujda;[(e)]Faculté des sciences, Université Mohammed V, Rabat; Morocco.
[36]CERN, Geneva; Switzerland.
[37]Enrico Fermi Institute, University of Chicago, Chicago IL; United States of America.
[38]LPC, Université Clermont Auvergne, CNRS/IN2P3, Clermont-Ferrand; France.
[39]Nevis Laboratory, Columbia University, Irvington NY; United States of America.
[40]Niels Bohr Institute, University of Copenhagen, Copenhagen; Denmark.
[41(a)]Dipartimento di Fisica, Università della Calabria, Rende;[(b)]INFN Gruppo Collegato di Cosenza, Laboratori Nazionali di Frascati; Italy.
[42]Physics Department, Southern Methodist University, Dallas TX; United States of America.
[43]Physics Department, University of Texas at Dallas, Richardson TX; United States of America.
[44]National Centre for Scientific Research "Demokritos", Agia Paraskevi; Greece.
[45(a)]Department of Physics, Stockholm University;[(b)]Oskar Klein Centre, Stockholm; Sweden.
[46]Deutsches Elektronen-Synchrotron DESY, Hamburg and Zeuthen; Germany.
[47]Lehrstuhl für Experimentelle Physik IV, Technische Universität Dortmund, Dortmund; Germany.
[48]Institut für Kern- und Teilchenphysik, Technische Universität Dresden, Dresden; Germany.
[49]Department of Physics, Duke University, Durham NC; United States of America.
[50]SUPA - School of Physics and Astronomy, University of Edinburgh, Edinburgh; United Kingdom.
[51]INFN e Laboratori Nazionali di Frascati, Frascati; Italy.
[52]Physikalisches Institut, Albert-Ludwigs-Universität Freiburg, Freiburg; Germany.
[53]II. Physikalisches Institut, Georg-August-Universität Göttingen, Göttingen; Germany.
[54]Département de Physique Nucléaire et Corpusculaire, Université de Genève, Genève; Switzerland.
[55(a)]Dipartimento di Fisica, Università di Genova, Genova;[(b)]INFN Sezione di Genova; Italy.
[56]II. Physikalisches Institut, Justus-Liebig-Universität Giessen, Giessen; Germany.
[57]SUPA - School of Physics and Astronomy, University of Glasgow, Glasgow; United Kingdom.
[58]LPSC, Université Grenoble Alpes, CNRS/IN2P3, Grenoble INP, Grenoble; France.
[59]Laboratory for Particle Physics and Cosmology, Harvard University, Cambridge MA; United States of America.
[60(a)]Department of Modern Physics and State Key Laboratory of Particle Detection and Electronics, University of Science and Technology of China, Hefei;[(b)]Institute of Frontier and Interdisciplinary Science and Key Laboratory of Particle Physics and Particle Irradiation (MOE), Shandong University, Qingdao;[(c)]School of Physics and Astronomy, Shanghai Jiao Tong University, KLPPAC-MoE, SKLPPC, Shanghai;[(d)]Tsung-Dao Lee Institute, Shanghai; China.
[61(a)]Kirchhoff-Institut für Physik, Ruprecht-Karls-Universität Heidelberg, Heidelberg;[(b)]Physikalisches Institut, Ruprecht-Karls-Universität Heidelberg, Heidelberg; Germany.
[62]Faculty of Applied Information Science, Hiroshima Institute of Technology, Hiroshima; Japan.
[63(a)]Department of Physics, Chinese University of Hong Kong, Shatin, N.T., Hong Kong;[(b)]Department of Physics, University of Hong Kong, Hong Kong;[(c)]Department of Physics and Institute for Advanced Study,

Hong Kong University of Science and Technology, Clear Water Bay, Kowloon, Hong Kong; China.
[64]Department of Physics, National Tsing Hua University, Hsinchu; Taiwan.
[65]IJCLab, Université Paris-Saclay, CNRS/IN2P3, 91405, Orsay; France.
[66]Department of Physics, Indiana University, Bloomington IN; United States of America.
[67(a)]INFN Gruppo Collegato di Udine, Sezione di Trieste, Udine;[(b)]ICTP, Trieste;[(c)]Dipartimento Politecnico di Ingegneria e Architettura, Università di Udine, Udine; Italy.
[68(a)]INFN Sezione di Lecce;[(b)]Dipartimento di Matematica e Fisica, Università del Salento, Lecce; Italy.
[69(a)]INFN Sezione di Milano;[(b)]Dipartimento di Fisica, Università di Milano, Milano; Italy.
[70(a)]INFN Sezione di Napoli;[(b)]Dipartimento di Fisica, Università di Napoli, Napoli; Italy.
[71(a)]INFN Sezione di Pavia;[(b)]Dipartimento di Fisica, Università di Pavia, Pavia; Italy.
[72(a)]INFN Sezione di Pisa;[(b)]Dipartimento di Fisica E. Fermi, Università di Pisa, Pisa; Italy.
[73(a)]INFN Sezione di Roma;[(b)]Dipartimento di Fisica, Sapienza Università di Roma, Roma; Italy.
[74(a)]INFN Sezione di Roma Tor Vergata;[(b)]Dipartimento di Fisica, Università di Roma Tor Vergata, Roma; Italy.
[75(a)]INFN Sezione di Roma Tre;[(b)]Dipartimento di Matematica e Fisica, Università Roma Tre, Roma; Italy.
[76(a)]INFN-TIFPA;[(b)]Università degli Studi di Trento, Trento; Italy.
[77]Institut für Astro- und Teilchenphysik, Leopold-Franzens-Universität, Innsbruck; Austria.
[78]University of Iowa, Iowa City IA; United States of America.
[79]Department of Physics and Astronomy, Iowa State University, Ames IA; United States of America.
[80]Joint Institute for Nuclear Research, Dubna; Russia.
[81(a)]Departamento de Engenharia Elétrica, Universidade Federal de Juiz de Fora (UFJF), Juiz de Fora;[(b)]Universidade Federal do Rio De Janeiro COPPE/EE/IF, Rio de Janeiro;[(c)]Universidade Federal de São João del Rei (UFSJ), São João del Rei;[(d)]Instituto de Física, Universidade de São Paulo, São Paulo; Brazil.
[82]KEK, High Energy Accelerator Research Organization, Tsukuba; Japan.
[83]Graduate School of Science, Kobe University, Kobe; Japan.
[84(a)]AGH University of Science and Technology, Faculty of Physics and Applied Computer Science, Krakow;[(b)]Marian Smoluchowski Institute of Physics, Jagiellonian University, Krakow; Poland.
[85]Institute of Nuclear Physics Polish Academy of Sciences, Krakow; Poland.
[86]Faculty of Science, Kyoto University, Kyoto; Japan.
[87]Kyoto University of Education, Kyoto; Japan.
[88]Research Center for Advanced Particle Physics and Department of Physics, Kyushu University, Fukuoka ; Japan.
[89]Instituto de Física La Plata, Universidad Nacional de La Plata and CONICET, La Plata; Argentina.
[90]Physics Department, Lancaster University, Lancaster; United Kingdom.
[91]Oliver Lodge Laboratory, University of Liverpool, Liverpool; United Kingdom.
[92]Department of Experimental Particle Physics, Jožef Stefan Institute and Department of Physics, University of Ljubljana, Ljubljana; Slovenia.
[93]School of Physics and Astronomy, Queen Mary University of London, London; United Kingdom.
[94]Department of Physics, Royal Holloway University of London, Egham; United Kingdom.
[95]Department of Physics and Astronomy, University College London, London; United Kingdom.
[96]Louisiana Tech University, Ruston LA; United States of America.
[97]Fysiska institutionen, Lunds universitet, Lund; Sweden.
[98]Centre de Calcul de l'Institut National de Physique Nucléaire et de Physique des Particules (IN2P3), Villeurbanne; France.
[99]Departamento de Física Teorica C-15 and CIAFF, Universidad Autónoma de Madrid, Madrid; Spain.
[100]Institut für Physik, Universität Mainz, Mainz; Germany.

[101]School of Physics and Astronomy, University of Manchester, Manchester; United Kingdom.
[102]CPPM, Aix-Marseille Université, CNRS/IN2P3, Marseille; France.
[103]Department of Physics, University of Massachusetts, Amherst MA; United States of America.
[104]Department of Physics, McGill University, Montreal QC; Canada.
[105]School of Physics, University of Melbourne, Victoria; Australia.
[106]Department of Physics, University of Michigan, Ann Arbor MI; United States of America.
[107]Department of Physics and Astronomy, Michigan State University, East Lansing MI; United States of America.
[108]B.I. Stepanov Institute of Physics, National Academy of Sciences of Belarus, Minsk; Belarus.
[109]Research Institute for Nuclear Problems of Byelorussian State University, Minsk; Belarus.
[110]Group of Particle Physics, University of Montreal, Montreal QC; Canada.
[111]P.N. Lebedev Physical Institute of the Russian Academy of Sciences, Moscow; Russia.
[112]National Research Nuclear University MEPhI, Moscow; Russia.
[113]D.V. Skobeltsyn Institute of Nuclear Physics, M.V. Lomonosov Moscow State University, Moscow; Russia.
[114]Fakultät für Physik, Ludwig-Maximilians-Universität München, München; Germany.
[115]Max-Planck-Institut für Physik (Werner-Heisenberg-Institut), München; Germany.
[116]Nagasaki Institute of Applied Science, Nagasaki; Japan.
[117]Graduate School of Science and Kobayashi-Maskawa Institute, Nagoya University, Nagoya; Japan.
[118]Department of Physics and Astronomy, University of New Mexico, Albuquerque NM; United States of America.
[119]Institute for Mathematics, Astrophysics and Particle Physics, Radboud University Nijmegen/Nikhef, Nijmegen; Netherlands.
[120]Nikhef National Institute for Subatomic Physics and University of Amsterdam, Amsterdam; Netherlands.
[121]Department of Physics, Northern Illinois University, DeKalb IL; United States of America.
[122](a)Budker Institute of Nuclear Physics and NSU, SB RAS, Novosibirsk;(b)Novosibirsk State University Novosibirsk; Russia.
[123]Institute for High Energy Physics of the National Research Centre Kurchatov Institute, Protvino; Russia.
[124]Institute for Theoretical and Experimental Physics named by A.I. Alikhanov of National Research Centre "Kurchatov Institute", Moscow; Russia.
[125]Department of Physics, New York University, New York NY; United States of America.
[126]Ochanomizu University, Otsuka, Bunkyo-ku, Tokyo; Japan.
[127]Ohio State University, Columbus OH; United States of America.
[128]Faculty of Science, Okayama University, Okayama; Japan.
[129]Homer L. Dodge Department of Physics and Astronomy, University of Oklahoma, Norman OK; United States of America.
[130]Department of Physics, Oklahoma State University, Stillwater OK; United States of America.
[131]Palacký University, RCPTM, Joint Laboratory of Optics, Olomouc; Czech Republic.
[132]Center for High Energy Physics, University of Oregon, Eugene OR; United States of America.
[133]Graduate School of Science, Osaka University, Osaka; Japan.
[134]Department of Physics, University of Oslo, Oslo; Norway.
[135]Department of Physics, Oxford University, Oxford; United Kingdom.
[136]LPNHE, Sorbonne Université, Université de Paris, CNRS/IN2P3, Paris; France.
[137]Department of Physics, University of Pennsylvania, Philadelphia PA; United States of America.
[138]Konstantinov Nuclear Physics Institute of National Research Centre "Kurchatov Institute", PNPI, St. Petersburg; Russia.

[139]Department of Physics and Astronomy, University of Pittsburgh, Pittsburgh PA; United States of America.
[140(a)]Laboratório de Instrumentação e Física Experimental de Partículas - LIP, Lisboa;[(b)]Departamento de Física, Faculdade de Ciências, Universidade de Lisboa, Lisboa;[(c)]Departamento de Física, Universidade de Coimbra, Coimbra;[(d)]Centro de Física Nuclear da Universidade de Lisboa, Lisboa;[(e)]Departamento de Física, Universidade do Minho, Braga;[(f)]Departamento de Física Teórica y del Cosmos, Universidad de Granada, Granada (Spain);[(g)]Dep Física and CEFITEC of Faculdade de Ciências e Tecnologia, Universidade Nova de Lisboa, Caparica;[(h)]Instituto Superior Técnico, Universidade de Lisboa, Lisboa; Portugal.
[141]Institute of Physics of the Czech Academy of Sciences, Prague; Czech Republic.
[142]Czech Technical University in Prague, Prague; Czech Republic.
[143]Charles University, Faculty of Mathematics and Physics, Prague; Czech Republic.
[144]Particle Physics Department, Rutherford Appleton Laboratory, Didcot; United Kingdom.
[145]IRFU, CEA, Université Paris-Saclay, Gif-sur-Yvette; France.
[146]Santa Cruz Institute for Particle Physics, University of California Santa Cruz, Santa Cruz CA; United States of America.
[147(a)]Departamento de Física, Pontificia Universidad Católica de Chile, Santiago;[(b)]Universidad Andres Bello, Department of Physics, Santiago;[(c)]Departamento de Física, Universidad Técnica Federico Santa María, Valparaíso; Chile.
[148]Department of Physics, University of Washington, Seattle WA; United States of America.
[149]Department of Physics and Astronomy, University of Sheffield, Sheffield; United Kingdom.
[150]Department of Physics, Shinshu University, Nagano; Japan.
[151]Department Physik, Universität Siegen, Siegen; Germany.
[152]Department of Physics, Simon Fraser University, Burnaby BC; Canada.
[153]SLAC National Accelerator Laboratory, Stanford CA; United States of America.
[154]Physics Department, Royal Institute of Technology, Stockholm; Sweden.
[155]Departments of Physics and Astronomy, Stony Brook University, Stony Brook NY; United States of America.
[156]Department of Physics and Astronomy, University of Sussex, Brighton; United Kingdom.
[157]School of Physics, University of Sydney, Sydney; Australia.
[158]Institute of Physics, Academia Sinica, Taipei; Taiwan.
[159(a)]E. Andronikashvili Institute of Physics, Iv. Javakhishvili Tbilisi State University, Tbilisi;[(b)]High Energy Physics Institute, Tbilisi State University, Tbilisi; Georgia.
[160]Department of Physics, Technion, Israel Institute of Technology, Haifa; Israel.
[161]Raymond and Beverly Sackler School of Physics and Astronomy, Tel Aviv University, Tel Aviv; Israel.
[162]Department of Physics, Aristotle University of Thessaloniki, Thessaloniki; Greece.
[163]International Center for Elementary Particle Physics and Department of Physics, University of Tokyo, Tokyo; Japan.
[164]Graduate School of Science and Technology, Tokyo Metropolitan University, Tokyo; Japan.
[165]Department of Physics, Tokyo Institute of Technology, Tokyo; Japan.
[166]Tomsk State University, Tomsk; Russia.
[167]Department of Physics, University of Toronto, Toronto ON; Canada.
[168(a)]TRIUMF, Vancouver BC;[(b)]Department of Physics and Astronomy, York University, Toronto ON; Canada.
[169]Division of Physics and Tomonaga Center for the History of the Universe, Faculty of Pure and Applied Sciences, University of Tsukuba, Tsukuba; Japan.
[170]Department of Physics and Astronomy, Tufts University, Medford MA; United States of America.

[171]Department of Physics and Astronomy, University of California Irvine, Irvine CA; United States of America.
[172]Department of Physics and Astronomy, University of Uppsala, Uppsala; Sweden.
[173]Department of Physics, University of Illinois, Urbana IL; United States of America.
[174]Instituto de Física Corpuscular (IFIC), Centro Mixto Universidad de Valencia - CSIC, Valencia; Spain.
[175]Department of Physics, University of British Columbia, Vancouver BC; Canada.
[176]Department of Physics and Astronomy, University of Victoria, Victoria BC; Canada.
[177]Fakultät für Physik und Astronomie, Julius-Maximilians-Universität Würzburg, Würzburg; Germany.
[178]Department of Physics, University of Warwick, Coventry; United Kingdom.
[179]Waseda University, Tokyo; Japan.
[180]Department of Particle Physics, Weizmann Institute of Science, Rehovot; Israel.
[181]Department of Physics, University of Wisconsin, Madison WI; United States of America.
[182]Fakultät für Mathematik und Naturwissenschaften, Fachgruppe Physik, Bergische Universität Wuppertal, Wuppertal; Germany.
[183]Department of Physics, Yale University, New Haven CT; United States of America.
[a] Also at Borough of Manhattan Community College, City University of New York, New York NY; United States of America.
[b] Also at CERN, Geneva; Switzerland.
[c] Also at CPPM, Aix-Marseille Université, CNRS/IN2P3, Marseille; France.
[d] Also at Département de Physique Nucléaire et Corpusculaire, Université de Genève, Genève; Switzerland.
[e] Also at Departament de Fisica de la Universitat Autonoma de Barcelona, Barcelona; Spain.
[f] Also at Department of Applied Physics and Astronomy, University of Sharjah, Sharjah; United Arab Emirates.
[g] Also at Department of Financial and Management Engineering, University of the Aegean, Chios; Greece.
[h] Also at Department of Physics and Astronomy, Michigan State University, East Lansing MI; United States of America.
[i] Also at Department of Physics and Astronomy, University of Louisville, Louisville, KY; United States of America.
[j] Also at Department of Physics, Ben Gurion University of the Negev, Beer Sheva; Israel.
[k] Also at Department of Physics, California State University, East Bay; United States of America.
[l] Also at Department of Physics, California State University, Fresno; United States of America.
[m] Also at Department of Physics, California State University, Sacramento; United States of America.
[n] Also at Department of Physics, King's College London, London; United Kingdom.
[o] Also at Department of Physics, St. Petersburg State Polytechnical University, St. Petersburg; Russia.
[p] Also at Department of Physics, Stanford University, Stanford CA; United States of America.
[q] Also at Department of Physics, University of Adelaide, Adelaide; Australia.
[r] Also at Department of Physics, University of Fribourg, Fribourg; Switzerland.
[s] Also at Department of Physics, University of Michigan, Ann Arbor MI; United States of America.
[t] Also at Dipartimento di Matematica, Informatica e Fisica, Università di Udine, Udine; Italy.
[u] Also at Faculty of Physics, M.V. Lomonosov Moscow State University, Moscow; Russia.
[v] Also at Giresun University, Faculty of Engineering, Giresun; Turkey.
[w] Also at Graduate School of Science, Osaka University, Osaka; Japan.
[x] Also at Hellenic Open University, Patras; Greece.
[y] Also at IJCLab, Université Paris-Saclay, CNRS/IN2P3, 91405, Orsay; France.
[z] Also at Institucio Catalana de Recerca i Estudis Avancats, ICREA, Barcelona; Spain.
[aa] Also at Institut für Experimentalphysik, Universität Hamburg, Hamburg; Germany.

[ab] Also at Institute for Mathematics, Astrophysics and Particle Physics, Radboud University Nijmegen/Nikhef, Nijmegen; Netherlands.
[ac] Also at Institute for Nuclear Research and Nuclear Energy (INRNE) of the Bulgarian Academy of Sciences, Sofia; Bulgaria.
[ad] Also at Institute for Particle and Nuclear Physics, Wigner Research Centre for Physics, Budapest; Hungary.
[ae] Also at Institute of Particle Physics (IPP), Vancouver; Canada.
[af] Also at Institute of Physics, Azerbaijan Academy of Sciences, Baku; Azerbaijan.
[ag] Also at Instituto de Fisica Teorica, IFT-UAM/CSIC, Madrid; Spain.
[ah] Also at Joint Institute for Nuclear Research, Dubna; Russia.
[ai] Also at Louisiana Tech University, Ruston LA; United States of America.
[aj] Also at Manhattan College, New York NY; United States of America.
[ak] Also at Moscow Institute of Physics and Technology State University, Dolgoprudny; Russia.
[al] Also at National Research Nuclear University MEPhI, Moscow; Russia.
[am] Also at Physics Department, An-Najah National University, Nablus; Palestine.
[an] Also at Physics Dept, University of South Africa, Pretoria; South Africa.
[ao] Also at Physikalisches Institut, Albert-Ludwigs-Universität Freiburg, Freiburg; Germany.
[ap] Also at The City College of New York, New York NY; United States of America.
[aq] Also at Tomsk State University, Tomsk, and Moscow Institute of Physics and Technology State University, Dolgoprudny; Russia.
[ar] Also at TRIUMF, Vancouver BC; Canada.
[as] Also at Universita di Napoli Parthenope, Napoli; Italy.
[*] Deceased